

A REALIZATION OF FIBER LOOP RING DOWN SPECTROSCOPY FOR GAS SENSING

M.Tech Thesis

*Submitted in partial fulfillment of the requirements for the award of the Degree of
Master of Technology in Electronics and Communication Engineering*

By

**APARAJEETA GUHA
(Registration No. : 304201500500009)**

**Under the guidance of
Prof. Dr. Rajiv Ganguly**

**Dean, University of Engineering and Management, Kolkata, India
&**

Dr. Tarun Kumar Gangopadhyay

**Senior Principal Scientist, Fiber Optics and Photonics Division, CSIR-Central Glass
and Ceramic Research Institute (CGCRI), Kolkata**

**Submitted
in**

**DEPARTMENT OF ELECTRONICS AND COMMUNICATION ENGINEERING
UNIVERSITY OF ENGINEERING AND MANAGEMENT
NEWTOWN, KOLKATA, INDIA**

MAY 2017

DEPARTMENT OF ELECTRONICS AND COMMUNICATION ENGINEERING

UNIVERSITY OF ENGINEERING AND MANAGEMENT
NEWTOWN, KOLKATA, INDIA



CERTIFICATE

This to certify that the work presented in this thesis entitled “A realization of fiber loop ring down spectroscopy for gas sensing” has been carried out in CSIR-Central Glass and Ceramic Research Institute, based on the bonafide dissertation of research work by Ms. Aparajeeta Guha (Registration No. : 30420150050009) towards the partial fulfillment of the requirements for the award of the Degree of Master of Technology in Electronics and Communication Engineering of University of Engineering and Management during the academic period of 2015-1017.

A handwritten signature in black ink, appearing to read "Rajiv Ganguly", is placed over a horizontal line.

Internal guide

Prof. Dr. Rajiv Ganguly
Dean, University of Engineering
and Management
Kolkata, India

Place: KOLKATA
Date: 03-05-2017



केन्द्रीय कांच एवं सिरामिक अनुसंधान संस्थान

(वैज्ञानिक तथा औद्योगिक अनुसंधान परिषद)

CENTRAL GLASS & CERAMIC RESEARCH INSTITUTE



(COUNCIL OF SCIENTIFIC AND INDUSTRIAL RESEARCH)

दिनांक/Dated:

CERTIFICATE

This is to certify that this project work entitled "*A realization of fiber loop ring down spectroscopy for gas sensing*" is a bonafide work of M.Tech. Project done by Miss Aparajeeta Guha (*Registration No. : 30420150050009*), under the guidance of Dr. Tarun Kumar Gangopadhyay, Senior Principal Scientist in Fibre Optics and Photonics Division, CGCRI, Kolkata, during the academic period 2016-2017, towards the partial fulfillment of the requirements for the award of Degree of Master of Technology in Electronics and Communication Engineering of University of Engineering and Management, Kolkata.

Supervising Guide
(Signature & Designation)

Tarun Kumar Gangopadhyay

(Dr. Tarun Kumar Gangopadhyay)
Senior Principal Scientist
Fibre Optics and Photonics Division
Central Glass and Ceramic Research
Institute(CGCRI),
CSIR, Kolkata-700032, India

196, राजा एस. सी. मल्लिक रोड, कोलकाता - 700 032, भारत, 196, Raja S. C. Mullick Road, Kolkata - 700 032 India
दूरभाष/Phone : निदेशक/ Director : 2473-5829 कार्यालय/Office : 2473- 3469/76/77/96, 2483-9245/46/47, 2483-7340/41/42/43/44/45/46, 2483-7349/50

DID Lines : 2483-8079/8082, ग्राम/Gram : GLASCERCH फैक्स/Fax : (033) 2473-0957, 2483 7339, 2483 8085

ई-मेल/E.MAIL: director@cgcri.res.in, वेबसाइट/Website : www.cgcri.res.in

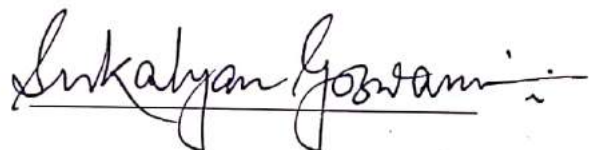
DEPARTMENT OF ELECTRONICS AND COMMUNICATION ENGINEERING

UNIVERSITY OF ENGINEERING AND MANAGEMENT
NEWTOWN, KOLKATA, INDIA



CERTIFICATE

This to certify that the work presented in this thesis entitled “A realization of fiber loop ring down spectroscopy for gas sensing” has been carried out in CSIR-Central Glass and Ceramic Research Institute, based on the bonafide dissertation of research work by Ms. Aparajeeta Guha (Registration No. : 304201500500009) towards the partial fulfillment of the requirements for the award of the Degree of Master of Technology in Electronics and Communication Engineering of University of Engineering and Management during the academic period of 2015-1017.



Head of the Department
Prof. Sukalyan Goswami
Department of Electronics and
Communication Engineering
University of Engineering and Management
Kolkata, India

DECLARATION

I hereby declare that the dissertation work presented in this thesis entitled "*A realization of fiber loop ring down spectroscopy for gas sensing*" is based on the work done by me towards to partial fulfillment of the requirements for the award of degree of Master of Technology in Electronics and Communication Engineering under the guidance of Dr. Tarun Kumar Gangopadhyay, Senior Principal Scientist, Fiber Optics and Photonics Division (FOPD), CSIR-Central Glass and Ceramic Research Institute (CGCRI), Kolkata.


Aparajeeta Guha
(Registration No. : 304201500500009)

ACKNOWLEDGEMENT

This project is by far one among the most significant accomplishments in my life and it would not have been possible without those who supported me and believed in me.

It is my privilege to express deep sense of gratitude to my project guide **Dr. Tarun Kumar Gangopadhyay**, Senior Principal Scientist, Fiber Optics & Photonics Division, CSIR-Central Glass & Ceramic Research Institute (CGCRI), Kolkata for his valuable help and inspiring guidance that facilitated me to complete this work successfully in time.

With great pleasure I express my sincere gratitude to **Dr. Rajiv Ganguly**, Professor and Dean, University of Engineering and Management, Kolkata for sanctioning permission and extending support and guidance to carry out the project work in CGCRI, Kolkata. I also thank the Director of CGCRI for giving me the opportunity to carry out my project work funded by CGCRI and DST (GAP0141) in this prestigious institute. My sincere thanks to all the Scientists and faculty in Fiber Optics & Photonics Division, CGCRI, for their invaluable support. I would like to extend thanks to **Mr. Jijo V Ittiarah** and **Mr. Debjit Dutta** JRF, FOPD, CGCRI, Kolkata, for their help and inspiration during this work.

My sincere thanks to all lecturers of the Department of Electronics and Communication Engineering, University of Engineering and Management, Kolkata, especially **Dr. Abir Chatterjee**, and **Mr. Subhajit Chatterjee**, **Mr. Soumen Banerjee** and **Mr. Sukalyan Goswami** for providing a solid background for my studies, and all other staff of the department including library, laboratory and administration in facilitating my studies.

I wish to thank my parents for their continuous moral support and help without which this accomplishment would not have been possible. Last but not the least I would like to thank the almighty **God** for all his blessings showering up on me during my daily life.

Aparajeeta Guha

TABLE OF CONTENTS

Abstract.....	1
List of Publications	3
List of Tables	4
List of Figures	5
Chapter 1	
 1.1 Introduction.....	7
 1.2 Physics of FLRDS	11
Chapter 2	
 2.1 An overview on recent applications of FLRDS in sensing Technology.....	13
Chapter 3	
 3.1 A study of experimental set up used in Fiber loop ring down Spectroscopy	26
 3.2. Brief description of different components of FLRDS set up in CGCRI.....	27
A. LASER.....	27
B. Coupler.....	27
C. High speed Detector.....	28
D. Optical modulator.....	29
E. Side polished fiber as Evanescent Access Block (EAB).....	29
Chapter 4	
 4. Theoretical simulations related to FLRDS.....	30
4.1. Time domain Analysis.....	30
4.2. Theoretical Simulations related to FLRDS.....	31
4.3. Effect of Coupler splitting ratio in FLRDS.....	35
Chapter 5	
 5. Electrical RC circuit to Model the FLRDS System.....	39
Chapter 6	
 6. Proposed set up for Gas sensing using FLRDS.....	42
6.1 Introduction.....	42
6.2 The proposed method and experimental set up for CO ₂ sensing using FLRDS.....	43
Chapter 7	
 7. Designing and analysis of Transimpedance amplifier for InGaAs Photodetector.....	46

7.1. Introduction.....	46
7.2 Design Methodology.....	47
7.3 Simulation.....	47
Chapter 8	
8. Conclusion.....	49
Reference.....	50
Appendix.....	52

Abstract

Cavity ring-down spectroscopy (CRDS) has proven to be a very sensitive gas-phase spectroscopic technique. It is suitable to record very weak transitions of abundant gases. Here, in the thesis the ring-down measurement principle to optical waveguides is presented. Fiber-loop ring-down spectroscopy (FLRDS) allows the measurement of absorption spectra of minute quantities of analyte. An optical fiber is wound into a loop using a fiber splice connector. In this technique a nanosecond laser light pulse is coupled into the fiber loop and the light pulses are detected using a photo detector. It is found that once the light is coupled into the fiber it experiences very little loss and the light pulses do a large number of round trips before their intensity is below the detection threshold. The characteristic ring-down time is obtained by exponential fitting of the envelope of the wave form.

The chapter 1 provides the introduction of CRDS and FLRDS. The advantages of FLRDS to basic fiber optic sensor (FOS) are revealed in terms of sensitivity and detection process. This chapter also describes the basic concepts regarding FLRDS.

The chapter 2 deals with detailed review of FLRDS scheme based on physical and chemical sensor employing different sensor elements.

In chapter 3, experimental setup for FLRDS is presented. Various electronic and optical components which are usually implemented in a FLRDS set up for successful execution of the experiment are discussed in details.

The chapter 4 gives a theoretical analysis of FLRDS system using MATLAB simulations. The time domain analysis of the FLRDS scheme has been carried out indicating the importance of each in sensing application. Further, a comprehensive study on the effect of coupler splitting ratio on the FLRDS output has been undertaken. The study is carried out in the presence and absence of sensor element within the optical path. These will help in the realization of the FLRDS.

In chapter 5, the FLRDS system is modeled using an electronic circuit. The corresponding analogy with the optical system is explained. The designed electronic circuit is also simulated using NI Multisim (version: 14.0) software. Finally the ring down time (RDT) is predicted from transient analysis of the designed circuit.

The chapter 6 presents the importance of gas sensing in present scenario. Finally a gas sensing technique and design using FLRDS is proposed and described in details.

In chapter 7, the designing of transimpedance amplifier is presented for the InGaAs photodetector proposed in the previous chapter. The related analysis and Multisim simulations are also presented in this chapter for better understanding.

Finally the thesis is concluded in chapter 8. The proposed gas sensor will help in realization and practical implementation of gas sensing using fiber loop ring-down spectroscopy with nano composite material.

List of Publications

- [1] Aparajeeta Guha and Tarun Kumar Gangopadhyay, "Theoretical analysis of fiber loop ring down spectroscopy for gas sensing" *International Conference on Electronics, Materials Engineering and Nano -Technology, 2017* organized by Institute of Engineering and Management, Kolkata.
(Presented and Accepted for IEEE digital Explore)

List of tables

Table. 1. Simulated values of ring down time corresponding to different loop losses.

Table 2. Output intensity of seven roundtrips of the fiber loop without the presence of sensor head in the optical path sensor head

Table. 3. Output intensity of seven roundtrips of the fiber loop with the presence of sensor head in the optical path sensor head

List of Figures

Fig. 1.1 Schematic diagram shows a typical CRDS setup with a laser source, photo detector, oscilloscope and two mirrors (m_1 and m_2) having large reflection coefficient. The presence of additional absorption in the cavity is detected by a shortening of the decay time constant (ringdown time). In the CRDS, the effective absorption path-length is readily increased more than 10,000-fold.

Fig. 1.2 Schematic of fiber loop ring down cavity consisting of laser source, photo detector and two couplers. The sensor head can be fabricated depending upon the applications.

Fig. 2.1 Schematic of the fiber loop system for trace gas sensing

Fig. 2.2 Ringdown pulses from 58m loop

Fig. 2.3 The effect of loop attenuation on ring down time

Fig. 2.4 Direct gas absorption cell.

Fig. 2.5 Setup of a linear fiber cavity. Two mirror elements, such as fiber Bragg. The light is injected through one of the mirrors and is detected behind the second mirror

Fig. 2.6 The structure of the experimental set up consists of a nitrogen laser, PMT and a fiber loop [10].

Fig. 2.7 Hydrogen gas is diffused into the fiber (at 30°) which caused absorption [12]

Fig. 2.8 Schematic for measurement of ring down time for detection of H₂ concentration [12]

Fig. 2.9 Measured additional loss during H₂ diffusion out of fiber cavity at 1590 nm [12]

Fig. 2.10 Fiber loop ring down using micro optic cell. This is basically a simplified as well as modified version of the first realization [8] of CRDS using fiber optic cavity [13].

Fig. 2.11 Schematic diagram of the passive continuous wave fiber cavity ring down system.

Fig. 2.12 Illustration of evanescent field [7]. It depicts how EF is distributed in a core and cladding of a fiber optic cable.

Fig. 2.13 Mammalian cancer cells that are adsorbed on the surface of the fiber taper and detected by FLRD [15].

Fig. 2.14 Schematic diagram of the fiber optic cavity ring-down apparatus as used for single cell detection of mammalian cancer cells [15].

Fig. 2.15 Schematic diagram of LPG cavity ringdown refractive index sensor.

Fig. 2.16 Fiber loop ring-down measurement setup using FBG cavity.

Fig. 2.17 Transmission spectrum of the LPG cavity in air and in decane [27]

Fig. 2.18 Schematic diagram of experimental setup for fiber loop cavity ring-down spectroscopy with a pair of LPGs.

Fig. 2.19. Schematic of EF-FLRD for index sensor [16].

Fig. 2.20. Refractive index based biosensor using a FLRD-EF sensing scheme [10] in which a bulk index based deoxyribonucleic acid (DNA) and bacteria sensing is depicted [17].

Fig. 2.21. Surface index-based label free DNA sensing of FLRDS-EF DNA sensor DNA(s1) selectively senses the target DNA (s2) but it has no response to the non matched DNA(s3) [17].

Fig. 2.22. Demonstration of the FLRD-EF sensor for the detection of bacteria [17]

Fig. 3.1 Experimental setup for fiber loop ring down spectroscopy

Fig. 3.2. Photograph of high splitting ratio coupler developed at CGCRI.

Fig. 4.1. Variation of pulse intensity with time for different loop losses.

Fig. 4.2. Variation of ringdown time with different loop losses (dB)

Fig. 4.3 Intensity as a function of number of round trips for different lengths of the loop.

Fig. 4.4 Ringdown time variation indicating the decay rate of core and cladding propagating through the optical fiber.

Fig. 4.5. Schematic diagram of FLRDS scheme for analyzing the effect of splitting ratio on the output

Fig. 5.1 RC circuit diagram of the used bi-exponential circuit with one decay time fixed at 10 μ s (top) and the second one adjusted to 90 μ s (bottom).

Fig. 5.2 Time domain measurement of the input response of the circuit to a square wave simulation.

Fig. 6.1 The proposed experimental set up for CO₂ sensing using FLRDS. The sensing mechanism takes place inside the gas cell.

Fig. 7.1 Active op-amp based transimpedance amplifier with photodiode This paper describes the design, implementation and application of TIA for InGaAs photodetector of TPP4NN3 series manufactured by Teradian.

Fig. 7.2. Transimpedance amplifier, with OPA656 drawn in Multisim; with Reverse light current 10 μ A and the feedback resistance 100k Ω

Fig. 7.3. AC analysis (a) gain v/s frequency and (b) phase v/s frequency

Fig. 7.4 The input and output signal from transient analysis with the selected OPAMP OPA656

Chapter 1

1.1 Introduction

Air is always around us, though we have never seen it but we can always feel its presence. The air on planet Earth is largely comprised of Nitrogen and Oxygen. The terrestrial lives directly take Oxygen from the atmosphere for breathing. If the world had no atmosphere, it would be very cold. The Earth's air helps to moderate the temperature and make it a habitable place for living organisms. Currently, the world is warming as the ratio of Carbon dioxide, Methane and other gases increases. These chemicals are called greenhouse gases because they cause the planet to warm up, just as a greenhouse does. Nowadays several industrial processes around the world are using and manufacturing highly dangerous substances, particularly toxic and incendiary gases [1]. This results in inevitable occasional escapes of such gases to the surrounding air, which gives rise to danger of risk to the industrial plant, its employees and people in the nearby places. Low concentration of toxic gas is also injurious to human health. Hence worldwide the incidents of asphyxiation, explosions, loss of life due to air pollution are increasing day by day [1]. Hence, the development of highly efficient and cost effective novel gas sensors is becoming an indispensable part for both scientific and industrial research. It is an important tool to prevent us from all such problems. Gas sensor has acquired a significant role in various fields like chemical and petrochemical industries, environmental pollution monitoring, engineering and scientific research institutes, automotive industries, medical institutes including hospitals, agriculture and food processing farms, etc. Gas detection is possible through a wide variety of techniques based on different materials and principles of operation. The most commonly used six categories are [1],

- 1) Optical Sensor
- 2) Electrochemical Sensor
- 3) Electrical Sensor
- 4) Mass-sensitive Sensor
- 5) Calorimetric Sensor
- 6) Magnetic Sensor

In this thesis the discussions and related experiments will be limited to a particular mechanism of optical gas sensing. Though each and every above mentioned process has its own advantages but the optical sensing methods possess unique advantages and easy access. By sensing, optically electromagnetic interference and the danger of explosion can be (almost) excluded. They also provide faster response (less than 1sec is possible) [1] and measurements can be made in real time without disturbing

the gas sample. An optical sensor contributes much higher sensitivity and selectivity than the other techniques. Optical gas sensors transform changes in optical phenomena which results from an interaction of analyte with the receptor part. It detects changes in electromagnetic waves during interactions with chemicals. In general, an optical sensing device is comprised of a light source, a wavelength selector, a recognition element for identification, interaction with the target gas, a transducer element to convert the recognition into a detectable signal and finally a detector to detect optical properties. These optical properties are converted to electrical signals [1]. Most commonly employed optical gas sensing techniques are chemiluminescence, absorption and fluorescence.

The use of optical fiber in various configurations of optical sensors makes the overall sensing system much more efficient and flexible in compared to other available mechanisms.

Cavity ring down spectroscopy (CRDS) is one of the most remarkable sensing technique, which is being used for over three decades due to its various advantages, such as immunity to electromagnetic interference, fast response, cheap, small footprint and high detection sensitivity [2]. CRDS has significantly higher detection sensitivity than conventional direct absorption techniques. The high sensitivity is due to intrinsic insensitivity of CRDS to laser power fluctuations and extremely long effective interaction path length (10KM), which is achieved using the optical cavity.

The basic concept of CRDS [3] technique is based on measuring the rate of absorption rather than the magnitude of absorption of a light pulse confined within a closed optical cavity. It is generally made of two highly reflective mirrors (with non zero transmission coefficient). When the laser is in resonance with the cavity mode, the intensity builds up in the cavity due to constructive interference.

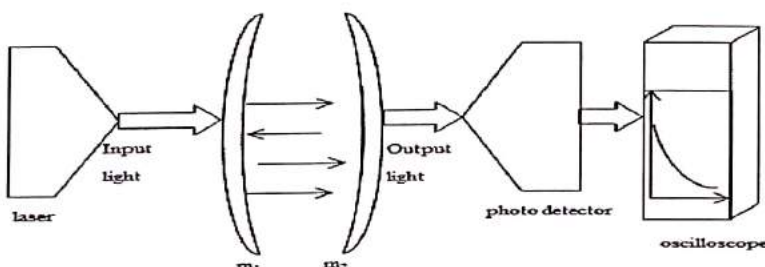


Fig. 1.1. Schematic diagram shows a typical CRDS setup with a laser source, photo detector, oscilloscope and two mirrors (m_1 and m_2) having large reflection coefficient. The presence of additional absorption in the cavity is detected by a shortening of the decay time constant (ringdown time). In the CRDS, the effective absorption path-length is readily increased more than 10,000-fold.

The laser is then turned off and exponentially decaying light intensity leaking from the cavity is measured. The decay time is inversely proportional to the losses in the cavity. The decay time is longer for the mirrors having higher reflectivity. The absorption coefficient can be determined from a comparison of the decay times for cavity with and without absorbers. Figure 1 depicts a typical setup, which includes a laser (light source), an optical cavity made up of two highly reflective mirrors (m_1 and m_2), a high speed photo detector and an oscilloscope with high sampling rate [2].

But an inherent limitation of CRDS is the usage of very large optical devices. It reduces the flexibility of the set up. Moreover it consists of mirrors having larger reflectivity, which are in general very expensive. Presently the CRDS technique is modified in Fiber Loop Ring down Spectroscopy (FLRDS). Being modified version of conventional CRDS method the FLRDS technique is blessed with the same advantages of CRDS as well as includes its own benefits. In the system of bulk cavity and mirrors, which were used previously replaced by the fiber loop. As in conventional CRDS, in Fibre-Loop Ring-Down Spectroscopy (FLRDS), the ringdown time (RDT) is also calculated as the ratio of the round trip time and all cavity losses. However, in FLRDS the different losses, and also the round trip time, are expressed differently with respect to the cavity length. In CRDS, a round trip is twice the length of the cavity. In FLRDS the length of the cavity equals one round trip. Furthermore, the round trip time is now dependent on the refractive index of the waveguide material, as the speed of light changes with the refractive index of the medium. In conventional CRDS, the refractive index change, due to the cavity medium, can usually be neglected. In connection with FLRDS, the term optical cavity should be explained properly for better understanding of the topic. An optical cavity is basically a resonator because the electromagnetic field inside the cavity becomes excited and increases amplitude by incident light at some particular resonant frequency [4]. Within the cavity a mode is a self producing wave, i.e. a wave that produces itself after a single round trip [5]. These modes are uniformly separated in frequency space by cavity Free Spectral Range (FSR), which is the reciprocal of the round trip time [4]. Another important parameter of optical cavity is finesse, i.e. basically represents the figure of merit for the cavity. It is defined by the ratio of the FSR over the full width at half maximum (FWHM) of the cavity resonances. A slower decay rate of signal within the cavity indicates lower optical loss within the resonator and vice versa. Fiber loop can be fabricated in two ways:

- (a) Linear fiber cavity , in which light is confined by fiber optic mirror such as fiber Bragg gratings (FBG)

Linear fiber cavity can be made by dielectric coatings on the fiber ends ,which acts as mirrors and in this method remarkably low loss per roundtrip is achieved experimentally

[6]. Most linear cavities are implemented using FBGs. Such FBGs are available for telecom wavelengths. This limits the usage of linear cavities.

(b) Fiber loop

Fiber is bent into a loop to form a ring cavity and fiber couplers of specific split ratio are used to inject light into the loop [Fig. 1.2] [6]. In comparison with the FBG cavity fiber loop is a broadband cavity. But as couplers are used in fiber ring method for a sensitive ring down time measurement we need to establish a balance between high loss per round trip and high coupling efficiency, because the couplers of high split ratio (99:1) can induce 2-4% loss per round trip [6].

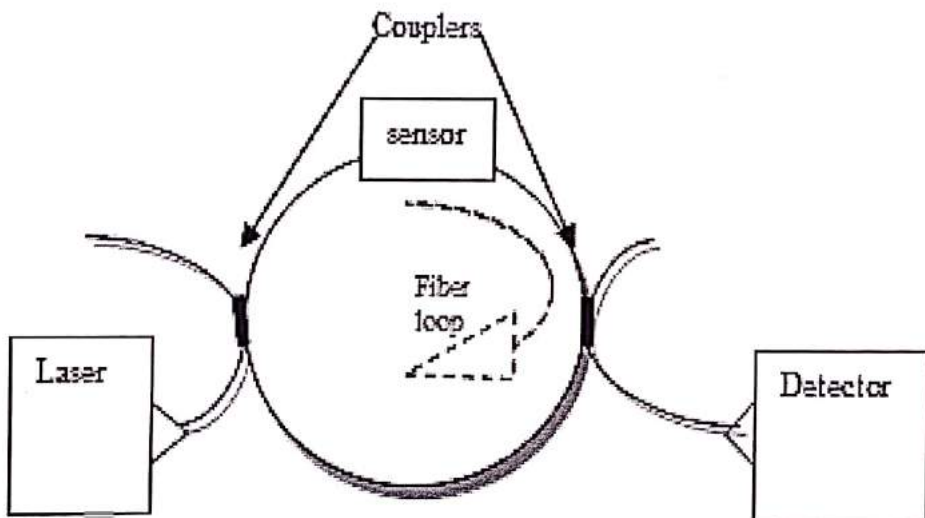


Fig. 1.2. Schematic of fiber loop ring down cavity consisting of laser source, photo detector and two couplers. The sensor head can be fabricated depending upon the applications.

Thus from all these discussion a direct comparison of the fiber loop sensor and the linear fiber cavity sensor can be concluded. The sensitivity is higher and detection limit is lower for linear fiber cavity system. This is likely due to slightly lower round trip losses and a larger light output at the detector. The large number of sensor head designs are now incorporated into fiber cavities shows the wide range of possible applications.

1.2. Physics of FLRDS

In a FLRDS setup a light pulse from the LASER gets coupled into a fiber loop. The light pulse then rings inside the loop for a number of round trips. In each round trip, a small fraction of light gets coupled out of the loop into a photo detector. The rest of the light travels in the fiber again and encounters internal fiber transmission losses. The output light identified by the detector experiences an exponential decay. Using the following equation this can be explained [3] as,

$$\frac{dI}{dt} = -\frac{IA_1c}{nL} \quad (1)$$

Where I is the light intensity at time t when the light source is switched off and a light pulse is injected into the fiber loop, A_1 is the total fiber transmission loss, c is the speed of light in vacuum, n is the averaged refractive index of the fiber loop and L is the total length of the loop. The fiber transmission loss includes the fiber absorption loss, the coupling losses, and the fiber scattering loss [3],

$$A_1 = \alpha L + L_c + \delta \quad (2)$$

Where, α is the wavelength dependent absorption coefficient for the fiber core material, L_c is the total coupling loss, and δ is the total fiber scattering loss. The temporal behaviour of light intensity is found from the solution of the equation (1) as,

$$I = I_0 e^{-\frac{cA_1t}{nL}} \quad (3)$$

Where, I_0 is the intensity of incident light. FLRDS being a time domain technique, the signal measured is found to be a time constant (decay constant, τ). Decay constant is the time taken, for the intensity of light to fall to $1/e$ times the initial intensity. This is basically called the ring down time (RDT). Ring down time is dependent on the loss mechanism within the loop. It is independent of intensity fluctuations and detector efficiency. The decay of light intensity is due to absorption and scattering. Ring down time is given as [3],

$$\tau_1 = \frac{nL}{cA_1} \quad (4)$$

Whenever a sensor head and some chemical are introduced within the fiber loop, further losses A_s (due to sensor head) and A_a (due to the chemical to be sensed) are also induced. Hence this phenomena results a noticeable decrement of RDT. The new RDT is given by [3],

$$\tau_a = \frac{nL}{c(A_1+A_a+A_s)} \quad (5)$$

If equations (3), (4) and (5) are solved, it will produce,

$$(A_a + A_s) = \frac{nL}{c} \left(\frac{1}{\tau_a} - \frac{1}{\tau_l} \right) \quad (6)$$

Where, τ_a is the ring down time due to induced loss for the introduction of both chemical (or gas) and sensor head within the loop. Now using the method of refractive index mismatch A_a can be determined easily just by, eliminating the effect of A_s .

Chapter 2

2.1 An overview on recent applications of FLRDS in sensing Technology

The development of the new spectroscopic technique cavity ring down spectroscopy (CRDS), was introduced by O'Keefe and Deacon [3] in the year 1988. Later in 2001 Stewart et al. [8] demonstrated slightly different sensing technique using FLRDS. Initially scientists have used FLRDS for detection of trace gases but afterwards it's being used as physical, chemical and even for biomedical and biological sensors till date.

In 2001, Stewart et al [8] was first to investigate and report the use of FLRDS for standoff sensing of methane in landfills, with the help of micro-optic gas cell of length 5 cm. They fabricated a fiber loop ring down system for the measurement of gas phase samples. They demonstrated detection of trace gases (CO_2 , CO , H_2S , and C_2H_2) by introducing a tiny air gap in the fiber cavity. A 5 cm open path gas cell within the fiber loop was fabricated for direct gas absorption. A schematic diagram for this approach is shown in Fig. 2.1. [8].

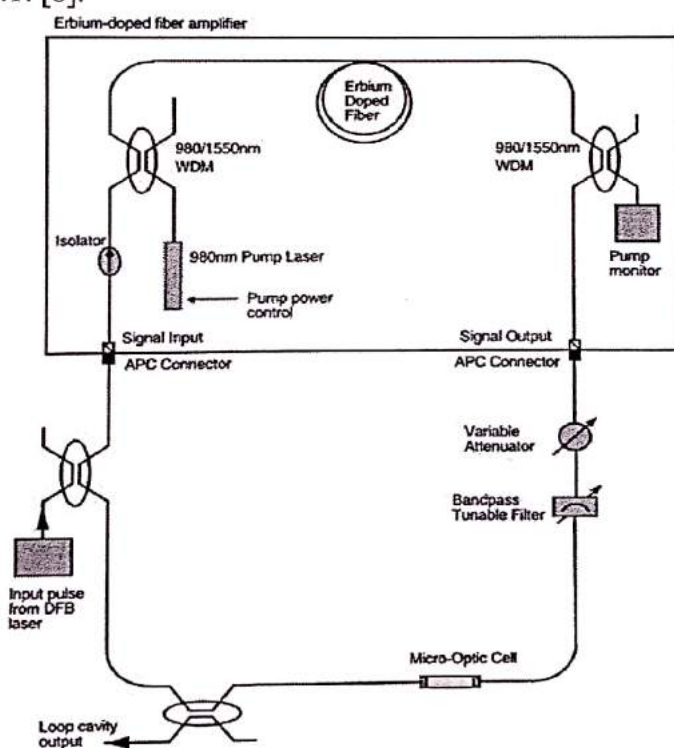


Fig. 2.1. Schematic of Fiber loop ring down spectroscopic system for trace gas detection [8]

Since a 1dB optical loss appeared due to the presence of the gap, the ring down times were very short, 100ns. To compensate large optical loss of the system, a 15-20m long Erbium doped fiber was introduced into the loop. The experimental set up consists of a fiber loop containing a certain length of

Erbium doped fiber that is pumped at 980nm with gain adjustments done above and below the threshold for operation in two type of region. The Erbium doped fiber amplifier (EDFA) was used in order to compensate for the very high losses that are expected to occur within the micro-optic gas cell. The loop is constructed from basic optical components i.e. SMF-28 fiber and includes a micro-optical gas cell that holds the particular traces of chemical for sensing. The intended application was the measurement of trace volume of gases which possess near infra ray absorption lines that lies within the gain bandwidth of Erbium doped fiber amplifier. In the original setup with a loop of 58m, the ring down time was extended up to $2.6\mu s$, giving the total round trip loss of 0.48dB [Figure.5-6] ($\sim 10.5\%$ loss). This was the first successful demonstration of fiber cavity ring down spectroscopy technique. Stewart et al showed that bulk cavity had to be minimum of 1m long to give rise to 5-10ns RDT, hence pulse width need to be less than 5ns to avoid effect of interference.

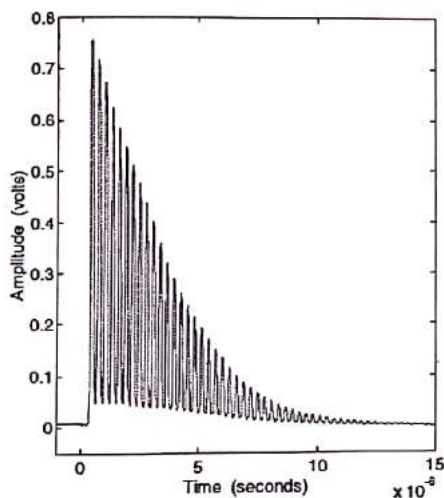


Figure. 2.2. Ringdown pulses from 58m loop [8]

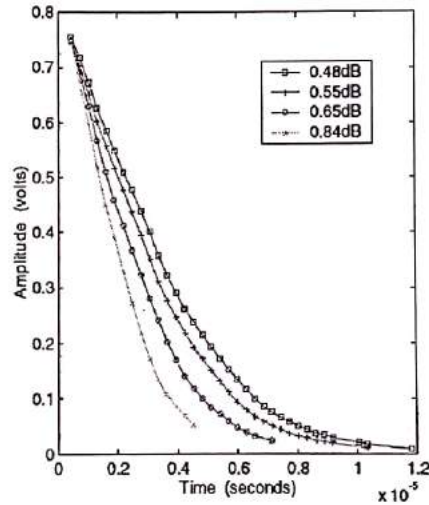


Figure. 2.3. The effect of loop attenuation on ring down time [8]

Whereas fiber based cavity can be several tens of meters long without keeping any constraints on the pulse width. But main drawback of this direct pass gas phase absorption approach was its low sensitivity because it had to compromise with the short path length (the gap) to get the effect of the ring down enhanced multiple pass (Fig. 2.4.).

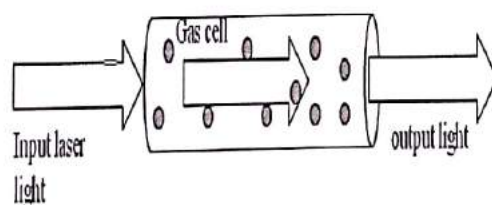


Fig. 2.4. Direct gas absorption cell.

In 2002, Gupta et al. [9] demonstrated a method for increasing the sensitivity of an intrinsic fiber optic sensor by introducing the sensing region within the high finesse optical cavity. This high finesse optical cavity was fabricated with the help of fiber Bragg grating (FBG) in both Germanium/Boron-co-doped photosensitive fiber and Hydrogen loaded corning SMF-28 fiber. Since the FBG is always normal to fiber axis and is within the fiber core, it is better than cavity formed by polished mirror ends. Optical losses within the cavity were determined by the Fabry Perot transmission spectra and CRDS. These losses were attributed to the absorption within the cavity. They also demonstrated enhanced sensitivity by fabricating an evanescent-wave access block (EAB) within the fiber cavity and inducing loss by alteration of refractive index of the external medium. The EAB has 6.9 cm length and it was made by asymmetric grinding. The variation in the fiber transmission was measured with respect to the external refractive index of the medium which is achieved by the help of glycerine-water mixture.

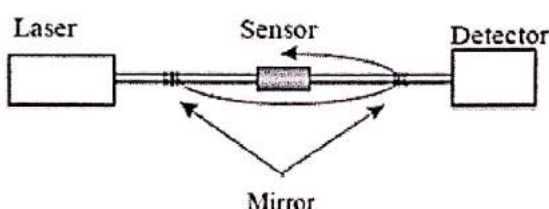


Fig. 2.5. Setup of a linear fiber cavity. Two mirror elements, such as fiber Bragg Gratings are incorporated into the fiber to form an optical cavity. The light is injected [9] through one of the mirrors and is detected behind the second mirror.

In the same year Brown et al [10] reported an FLRDS sensor in which a solution of organic dye was placed in between the ends of the optical fiber instead of an index matching liquid. The experimental set up consists of a Nitrogen laser pumped dye laser with a band width of about 0.05 nm and an energy of 50-200 mJ/pulse. The focused laser pulse was then coupled into the optical fiber loop ~2-77m at a bend of the fiber ~ 50 mm cores, 125 mm including the cladding. A photomultiplier tube (PMT) placed at a minimum distance of about 50 cm from the excitation region of the fiber monitored the scattered light. The PMT was gated to begin detection after 270 ns after the arrival of the laser pulse to avoid saturation by the initial round trips which were very intense due to the influence of the stray light and the light coupled into the fiber jacket other than the fiber core. An absorption spectrum of 7×10^{-15} mol of the dye1, 1'-diethyl-4, 4'-dicarbocyanine iodide in 7×10^{-12} L of dimethylsulfoxide was recorded. The figure shows the structure of the experimental set up. A nitrogen laser is pumped with a bandwidth of about 0.05 nm, with a width of 7 ns and energy of 50–200 mJ/pulse. The mildly focused output of this laser was coupled into the optical fiber-loop of length 2–77 m at a bend ($r=53$ cm) of the fiber (50 mm core, 125 mm) including the cladding. A photomultiplier tube (PMT) at min. 50 cm from the excitation region along the fiber monitored scattered

light at a similar bend. The PMT was gated to begin detecting 270 ns after laser pulse to avoid saturation by the initial round trips which were highly intense—likely from stray light and light coupled into the fiber core. A single laser shot typically results in the detection of about 50 to 200 photons distributed over all round trips [28].

In 2003, Zhaoguo Tong et al. [11] created a new sensor head for FLRDS sensor in which a crude 47mm channel in polydimethylsiloxane (PDMS) polymer was fabricated between the fiber end facets and the dye 1, 1'-diethyl-4, 4'-dicarbocyanine iodide~DDCI was introduced into the channel. The experimental setup employed a dye laser of 7ns, 50-200mJ/pulse and 800nm wavelength which was directed into the fiber optic loop. A gated PMT was used to detect the photons scattered from the fiber core and the cladding after a delay of about 250ns. The length of the fiber loop selected was about 11m and over 120 roundtrips were carried out so that the overall path length becomes 1.3Km. The experimental setup of Zhaoguo Tong et al. was similar to the set up of Brown et al [10] [Fig. 2.7.]. But here the RDT was determined to be $1.73\mu\text{s}$ for the modes coupled into the fiber core and 245ns for that in the cladding. From the concentration dependence of RDT the sample volume was determined as 700pL and the detection limit as about 10^{-12}mol , or $7 \times 10^{-8}\text{g}$ of DDCI. Characterization of the optical waveguides and connectors were also performed.

A novel type of fiber optic cavity sensor [12] for hydrogen diffusion into and out of the fiber was presented by Vogler et al. [12] in the year 2003. They implemented this scheme in a silicon based single mode fiber by exposing hydrogen at normal pressure. A 10m long fiber cavity ring down sensor for hydrogen diffusion [Fig. 2.8] was adopted. This approach claimed that it has the potential for remote sensing of any kind of losses experienced by the fiber and for the situations where the measurement is required with a short duration of time the schematic diagram of their set up is drawn in Figure 10.

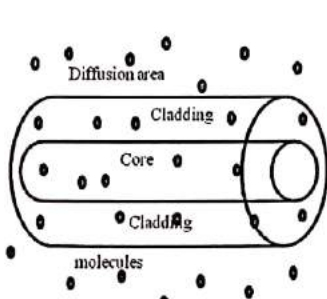


Fig. 2.7. Hydrogen gas is diffused into the fiber (at 30°) which caused absorption [12]

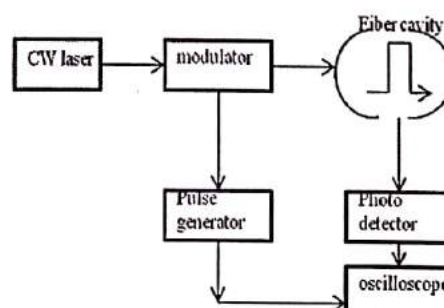


Fig. 2.8. Schematic for measurement of ring down time for detection of H₂ concentration [12]

This scheme of sensing also asserted an appreciable increase of additional optical loss due to diffused hydrogen molecules in silica in a wavelength range

of 1560-1600 nm [Fig. 2.9.]. The result showed an induced maximum additional loss of 1.2dB/km at 1586 nm. The difference of ring down times before and after the diffusion of gaseous hydrogen is found to be 3.5 μ s and the measured ring down time during the diffusion showed good agreement with theoretical values. One can determine the diffusion coefficient of hydrogen in silica, simultaneously with this setup. This is an added advantage of this model. In this case they found it to be $3.02 \pm 0.07 \times 10^{-15} \text{ m}^2/\text{s}$ at 30°C [12].

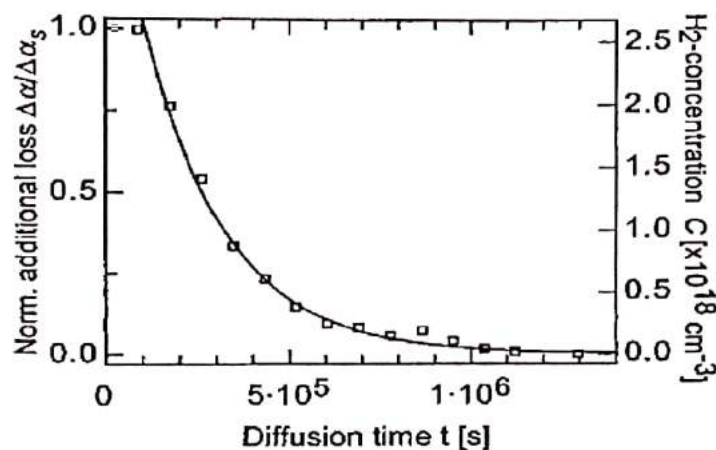


Fig. 2.9. Measured additional loss during H_2 diffusion out of fiber cavity at 1590 nm [12]

In 2004, George Stewart et al. [13] reported on loss compensation using active cavities amplifiers which permits the use of open path micro-optic cells. This was an extension of their previous research of year 2001. The configuration was simpler than the former because they applied combination of both lasing action and ring down in a single loop. The presence of lasing action within the loop gave rise of high finesse to the cavity. The schematic of the improved approach is depicted in Fig. 2.8. The experimental system consist a 5-10 m length of Erbium-doped fiber pumped at 980nm to provide gain along with a typical fiber loop cavity of 30-60 m. A distributed feedback laser source at 1532.8 nm wavelength is used to couple ~200ns pulse into fiber loop cavity to produce ring down signal. The gain obtained from the Erbium doped fiber section could be used to balance a large loop attenuation of ~20 dB. RDT of 2.5 ms were observed that were subsequently improved to ~10 ms. RDT can be extracted to several hundred microseconds by using gain-clamped cavities, but accuracy and repeatability is limited due to relaxation oscillations and system drift.

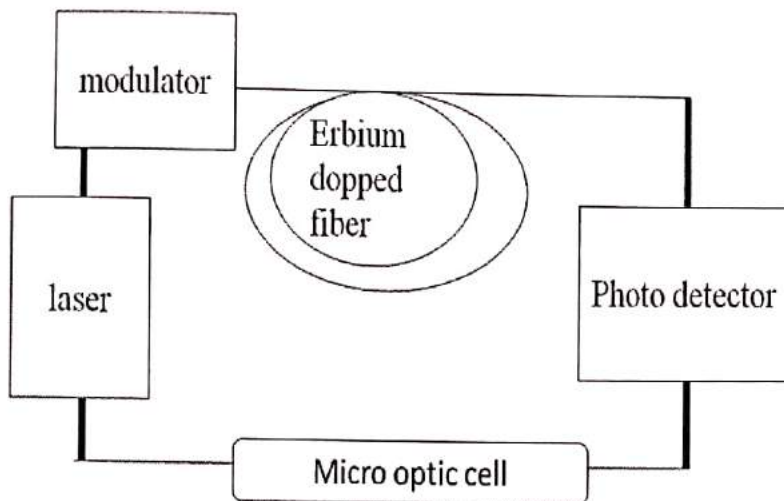


Fig. 2.10. Fiber loop ring down using micro optic cell. This is basically a simplified as well as modified version of the first realization [8] of CRDS using fiber optic cavity [13].

In 2004, Tarsa et al. presented a cavity ring-down spectroscopy (CRDS) for fiber optic sensing[20]. The experimental setup shown in the Fig. 2.11. The experimental setup consist of 2.2 km length single mode fiber, couplers with 99:1 splitting ratio, a pulsed laser source with a power of 10mW, external cavity diode laser (ECDL) with a peak wavelength of 1550 nm. The broad tuning range of ECDL was used for evanescent wave sensing spectra of molecular absorption band. The variation of resonator output with respect to ring down times were analysed which follows an exponential decay. The cavity decay time depends upon round trip time of cavity (t_r),cavity length (L), absorption coefficient(α) of species contained with the insertion and coupling loss of coupler ($2L_{coupler}$), transmission loss of fiber(L_{fiber}), fusion splice loss(L_{splice}), insertion loss of tapered sensing region(L_{taper}), loss due to external absorber in evanescent wave field(L_{abs}).

$$\tau = t_r / (2L_{coupler} + L_{fiber} + L_{splice} + L_{taper} + L_{abs}) \quad (1)$$

The output of the resonator can be described as a function[20],

$$F(t) = F(t_0)R^{\ln t(t-t_0)/t_r} \quad (2)$$

Where R is the resonator loss, t_0 is the time at which the laser is switched off, and t_r is the round trip time of the resonator.

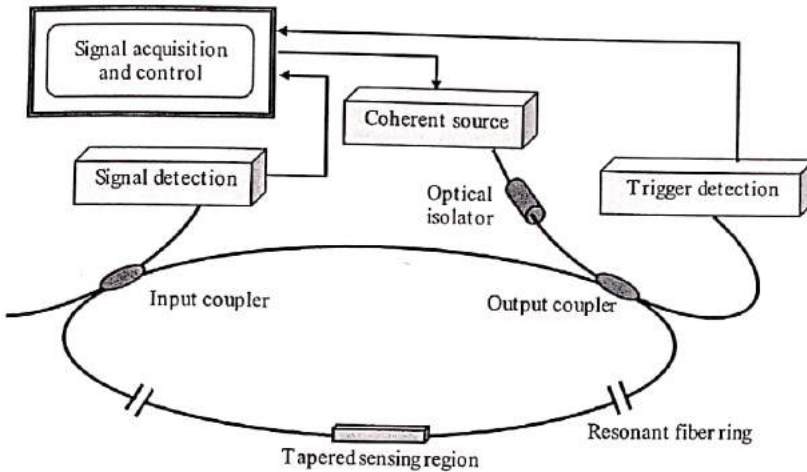


Fig. 2.11. Schematic diagram of the passive continuous wave fiber cavity ring down system.

Using light source with 1532.5nm in a non-interacting medium the minimum detectable concentration of 1-octyne in near-infrared absorption was $0.049\%/(Hz)^{1/2}$. The minimum detectable loss was $0.0.017\%/(Hz)^{1/2}$. The minimum sensing levels were found using Distributive feedback laser (DFB) laser.

FLRDS is a uniform time domain sensing scheme and hence evanescent field (EF) absorption and scattering can be adopted into this sensing platform [11] for the development of different sensors. EF-FLRD is a relatively new hybrid technique [7] in which a part of fiber is straightened to form a high finesse fiber ring down resonator to utilize EF absorption. In this case instead of leaving a gap in the fiber loop (which itself introduces loss) [7] EF-FLRD is used directly for sensing. Basically the refractive index of the measured medium approaches that of cladding and if a short region of cladding is removed from the optical fiber or the cladding is made thinner by tapering or side polishing, the evanescent field can be analysed as shown in Fig. 2.12.

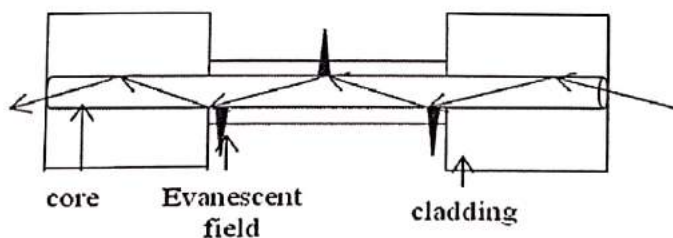


Fig. 2.12. Illustration of evanescent field [7]. It depicts how EF is distributed in a core and cladding of a fiber optic cable.

Since the evanescent wave interacts with surrounding medium, the fiber loop loss increases due to absorption and scattering. All the losses which are introduced due to EF-FLRD are determined by measuring the ring down time [7].

The Figure. 2.13. shows the image of the mammalian cancer cells attached to the surfaces of poly-D-lysine (PDL) coated taper single mode fiber (SMF) [15]. In the year 2004 Tarsa et al. also reported single-cell sensitivity arising from optical scattering of evanescent field surrounding the fiber. The schematic of measurement setup is depicted in Fig. 2.14.

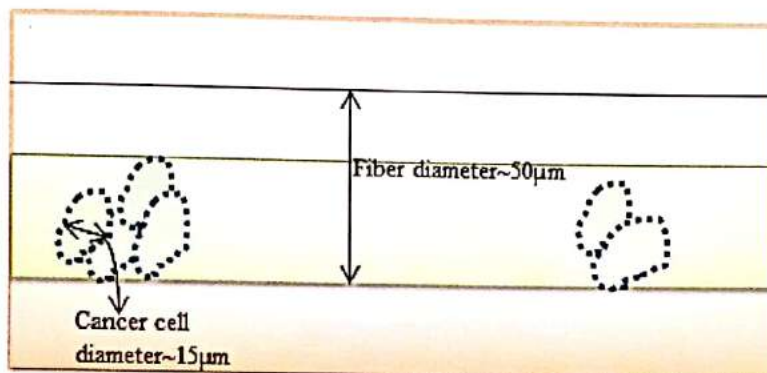


Fig. 2.13. Mammalian cancer cells that are adsorbed on the surface of the fiber taper and detected by FRLD [15].

This process claimed that by implementing molecular recognition technology the selectivity of the system can be enhanced. This would be possible by allowing highly sensitive real time detection of unlabeled splices by measuring the optical scattering. They used a fiber taper (10mm long) with a waist diameter of 25 μm. They coated the fiber with PDL to form an attaching substrate on the bare fiber surface so that the cells could then be effectively bonded to PDL chemically. The motive was to achieve the change in RI by the target cells within the interface between the taper surface and the coatings. Hence the resultant EF scattering losses are collected. Ultimately they got a linear behavior of RDT with cell count as a result.

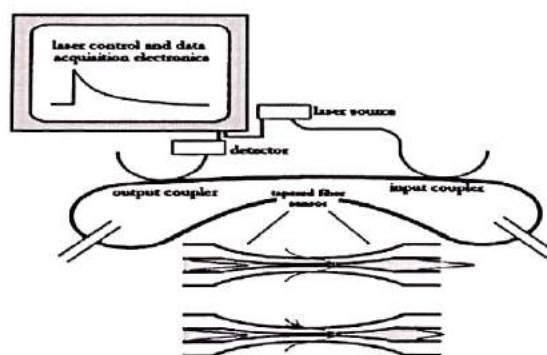


Fig. 2.14. Schematic diagram of the fiber optic cavity ring-down apparatus as used for single cell detection of mammalian cancer cells [15].

A standard error of $0.044\mu\text{s}$ was found from over 200 ring down events and the change in ring down time due to EF scattering of single cell was $0.23\mu\text{s}$ [15].

In 2008, N.Ni *et al.* presented a long period grating (LPG) cavity ringdown refractive index sensor in a fiber loop [25]. The experimental set up shown in the Fig. The fiber cavity was composed by two optical fiber couplers (Coupler 1 and 2) and a long segment of fiber. An LPG (period = 300m , the transmission loss was -22.4 dB at resonant wavelength 1580.2nm) was inserted into the fiber cavity, followed by a variable optical attenuator to adjust the total loss in the fiber cavity (in this scheme, the total loss composed of the transmission loss of the LPG, the attenuation loss from the variable attenuator and other residual loss such as fiber loss and component insertion losses). A tunable gain erbium-doped fiber amplifier (EDFA) was applied to provide a gain for compensating the large total loss in the fiber cavity. An FBG filter with full-width at half-maximum of 0.02 nm was connected in cascade behind the EDFA to minimize the undesirable amplified spontaneous emission powers brought by the EDFA. The CRD delay time and the LPG transmission loss changes with the LPG ambient refractive index. In their experiment the decay time remains invariable by adjusting the attenuation loss of the variable attenuator. The total loss was compensated and the net loss remains constant. The sensitivity of this sensor was evaluated by detecting the various decays at different ambient refractive indices.

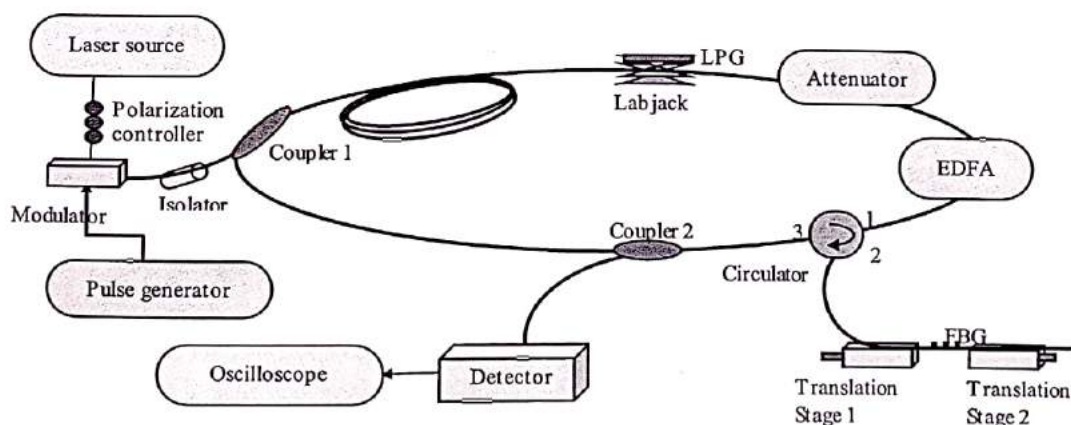


Fig.2.15. Schematic diagram of LPG cavity ringdown refractive index sensor.

In 2009, Kaiming Zhou *et al.* proposed a novel all-fiber cavity ringdown spectroscopy technique where a tilt fiber Bragg grating (TFBG) or long period grating (LPG) in the cavity provides sensitivity to surrounding medium [26]. With the aid of an evanescent wave induced by a TFBG, a novel fiber cavity ring down spectroscopy technique was demonstrated. The experimental setup is shown in Fig. 2.15.

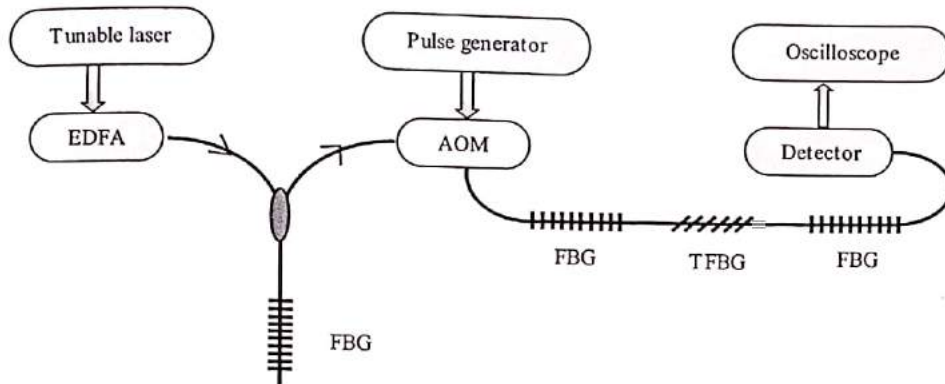


Fig. 2.16. Fiber loop ring-down measurement setup using FBG cavity.

The influence of splicing when the TFBG has to be spliced into the cavity is characterised. The insertion of TFBG in the middle of cavity causing the ring down time to reduce to 220 ns even though the splicer indicated 0dB loss. Thus the influence from splicing in the cavity is not trivial. An extra 10m fiber was spliced with the TFBG in the cavity and 3 splicing points were therefore introduced. When the TFBG is in air, the loss is huge and no decay curve could be observed because the spectral feature of the TFBG is just at the working wavelength.

In 2009, S. Pu *et al.* demonstrated a fiber loop ringdown spectroscopy with a Long Period Grating (LPG) cavity[27]. The transmission spectrum of the LPG cavity is compared when it is immersed into decane solution and without decane solution. A large spectral shift because the refractive index changes from 1 to 1.412 is observed. The spectral shift is negligible but its refractive index is 1.417. After that the LPG cavity is immersed in 1-octane solution as shown in Fig. 2.17. The experimental setup is shown in Fig. 2.18.

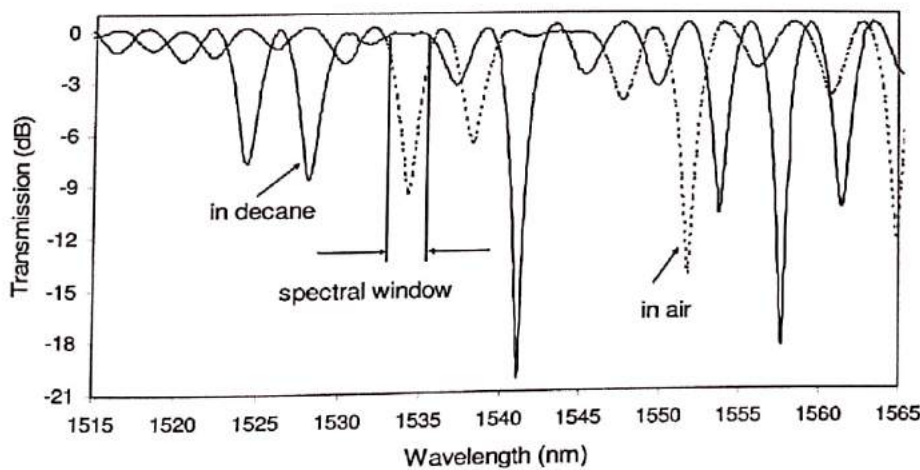


Fig. 2.17. Transmission spectrum of the LPG cavity in air and in decane [27]

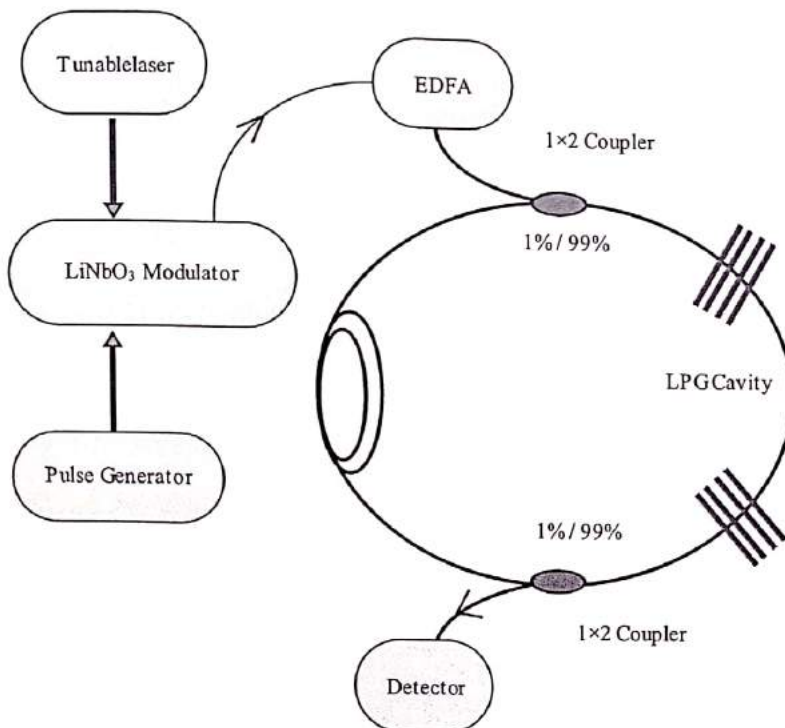


Fig. 1.18. Schematic diagram of experimental setup for fiber loop cavity ring-down spectroscopy with a pair of LPGs.

Single mode fiber (SMF-28) is used to make the fiber loop and a continuous wave laser as light source. The laser source was intensity modulated at 100 KHz with a LiNbO₃ modulator. The ringdown time is measured when the LPG cavity immersed into 100% decane and 40% 1-octane in decane. The large length of the LPG cavity giving more chances to the evanescent wave interaction, through that way one can improve the potential of the chemical sensor using LPG fiber cavity.

In 2010, Chuji Wang et al [16] reported a method of improving the sensitivity of EF index sensor by more than tenfold without employing any chemical immobilization or any delicate optical elements in the sensor head. Here the sensing element is the partial etched unclad single mode fiber. Fabrication of the sensor head is usually achieved by etching one end of the smaller section of optical fiber loop with 48% HF solution. The process is simultaneously monitored by FLRDS technique. Then this sensor head is immersed in the desired liquid having RI has to be found out. The sensor was then tested for two certified index oil which have RI of 1.3298 and 1.4389 at room temperature. The sensing was achieved on the basis of the RDT of fiber loop. The schematic of experiment is explained in the following figure.

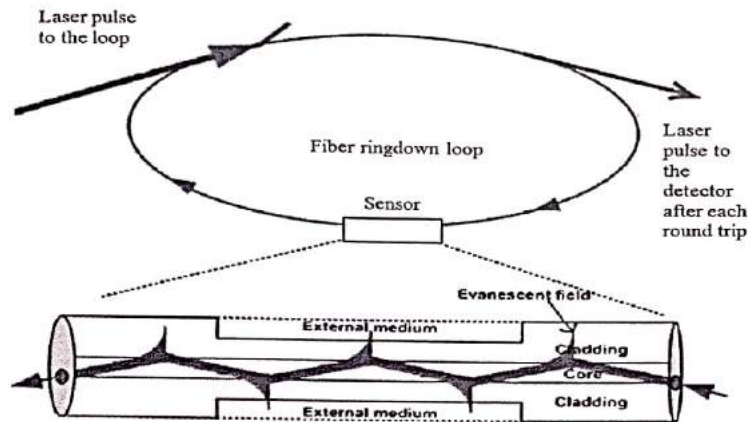


Fig. 2.19. Schematic of EF-FLRD for index sensor [16].

Chuji Wang et.al [17] in the year 2011 demonstrated a new type of refractive index based biosensor using a FLRD evanescent field (FLRD-EF) sensing scheme [10] in which a bulk index based deoxyribonucleic acid (DNA) and bacteria sensing is presented. They used a 24 cm long section of the fiber and a plastic jacket of that particular part was removed within a 48% hydrofluoric (HF) acid solution and that part of the fiber in contact with acid was etched away. As the EF propagating through the cladding starts to leak out of the medium, the observed RDT begins to decrease due to the increment of the optical loss. The resultant RDT was 4 and 5 μ s with optical loss of almost 0.05dB before and after the etching process. They investigated for three different DNA samples (26 base pairs single strand DNA(s1), 26 base another pair of single strand with different sequence (s2) and a combination of s1 and s2 with 26 base pair and double strand (s3) DNA). Fig. 2.20. illustrates the basic interrogation scheme [17].

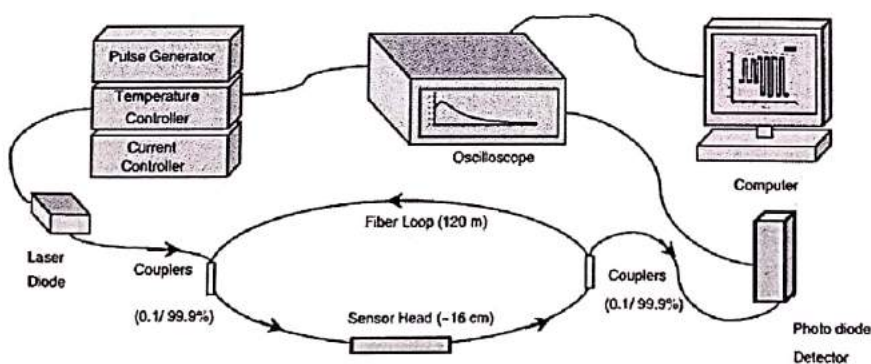


Fig. 2.20. RefRACTIVE index based biosensor using a FLRD-EF sensing scheme [10] in which a bulk index based deoxyribonucleic acid (DNA) and bacteria sensing is depicted [17].

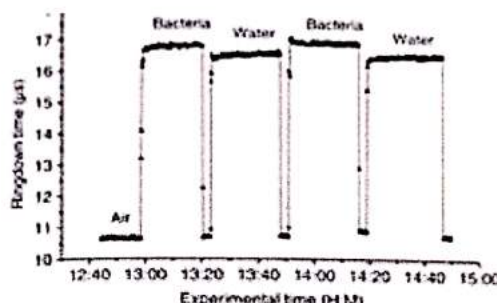


Fig. 2.21. Surface index-based label free DNA sensing of the FLD-EF sensor. The probe DNA(s1) selectively senses the target DNA (s2) but it has no response to the non matched DNA(s3) [17].

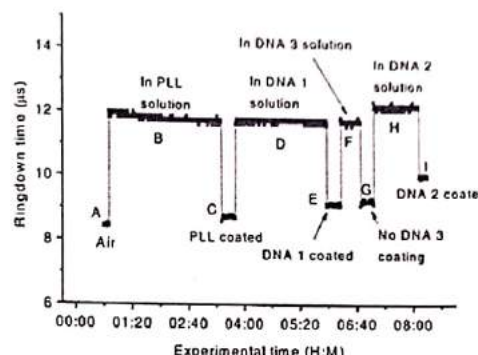


Fig. 2.22. Demonstration of the FLD-EF sensor for the detection of bacteria [17]

Thus from all these discussion a direct comparison of the fiber loop sensor and the linear fiber cavity sensor can be concluded. The sensitivity is higher and detection limit lower for linear fiber cavity system. This is likely due to slightly lower round trip losses and a larger light output at the detector. The large number of sensor head designs are now incorporated into fiber cavities shows the wide range of possible applications. The insensitivity to fluctuations in the light source output and detector response is particularly attractive features of any FLD method, including the potential to reduce operating costs and calibration for fiber sensor systems [18]. A fiber cavity may not always help to increase the sensitivity of the sensor system; hence in such situations one must carefully consider the sensor properties. For example, the insertion loss of the sensor head, i.e., its loss in the absence of analyte, may severely limit the sensitivity and detection limit [6]. This method of FLD has enough potential to be utilized as an efficient gas sensor. In the next section how the fiber loop ring down spectroscopy can be employed for effective gas sensing is explore.

Chapter 3

3.1 A study of experimental set up used in Fiber loop ring down Spectroscopy

The experimental setup for FLRDS in our lab at CGCRI, is consists of Agilent communication band laser having tunable wavelength from 1525nm to 1575nm, Pulse generator, Modulator having high bandwidth of 10 Gbps, couplers having high splitting ratio (99:1), Evanescent Access Block (EAB), a photo detector having response in picoseconds and a high bandwidth oscilloscope. Fiber loop is made from corning single mode fiber SMF28 having desirable length. Very high precision wavelength meter is also attached as an extra element. The existing experimental setup for FLRDS is shown in Fig.

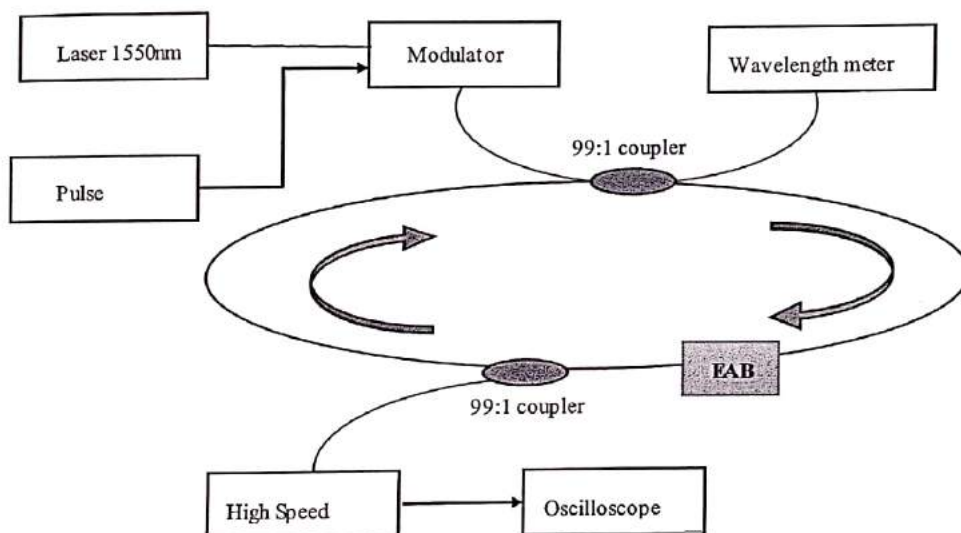


Fig. 3.1. Experimental setup for fiber loop ring down spectroscopy

3.2. Brief description of different components of FLRDS setup in CGCRI

A. LASER source

In our lab at CSIR-CGCRI, a tunable laser source (Agilent 81689B) is used. A tunable laser is a laser whose wavelength of operation can be altered in a controlled manner. This module operates in the C-band from 1525 nm to 1575 nm. Line width is around 20MHz. Output power is greater than 6 dBm and minimum output power is -3dBm. Output of the laser source is equipped with either standard single-mode fiber or Panda type polarization maintaining fiber. Tuning speed is typically greater than 50nm/s. As this laser is tunable with continuous output power, it is the most flexible for the test of optical amplifiers, DWDM components as well as for the test of complete DWDM systems. Wavelength scan function is possible by continuous sweep through full wavelength range. Wavelength-tunable laser sources have many applications. In spectroscopy, a wavelength-tunable laser with narrow optical bandwidth can be used for recording transmission or absorption spectra with very high frequency resolution. So this laser source is well suited for FLRDS application.

B. Coupler

In FLRDS, a different approach for coupling light into the fibre-loop than in traditional CRDS (which relies on the very small transmission of one of the mirrors) is needed. Couplers at different wavelengths are developed in our lab at CGCRI. They are constructed by fusing and tapering two fibers together. This method provides a simple, rugged, and compact method of splitting and combining optical signals. Unfortunately, couplers, like most other optical devices when spliced into a fibre cavity, introduce an insertion loss. For example, a coupling ratio of 99% : 1% does not mean that the total transmitted light at both outputs of the coupler adds up to 100% of the incident light, as couplers have an insertion loss of about 2% to 4%, and the rest of the intensity is split according to the coupling ratio. Therefore, when using fibre couplers, the insertion loss has to be taken into account. Fused couplers are used to split optical signals between two fibers, or to combine optical signals from two fibers into one fiber. Conventional fused fiber machine consisting of two chucks, which can hold a pair of stripped SM fiber and can move along a slide. Both chucks are attached to precision stepper motors for pulling of the fiber. Fusion is applied by a gas torch or by a ceramic heater. During the pulling process optical power is launched into one of the fiber and monitored in both of the output fiber. Fusion and pulling of the fiber can done up to the pre-determined values of optical power. All the process is controlled by special software with a graphical user interface. A photograph of 95:5 ratio coupler developed and packaged at CGCRI is shown in Fig. 3.2.

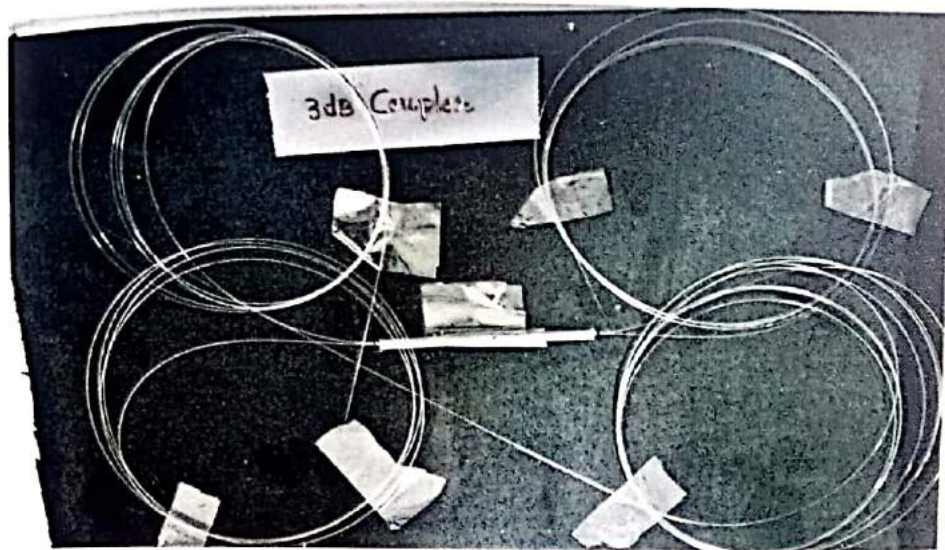


Fig. 3.2. Photograph of high splitting ratio coupler developed at CGCRI. [20]

C. High speed Detector

Photodetectors are devices used for the detection of light, in most cases of optical powers. Photodiodes are semiconductor devices with a p-n junction or p-i-n structure (i = intrinsic material) (p-i-n photodiodes), where light is absorbed in a depletion region and generates a photocurrent. Such devices can be very compact, fast, highly linear, and exhibit high quantum efficiency and a high dynamic range, provided that they are operated in combination with suitable electronics. A particularly sensitive type is that of avalanche photodiodes, which are sometimes used even for photon counting. Phototransistors are similar to photodiodes, but exploit internal amplification of the photocurrent. They are less frequently used than photodiodes.

Depending on the application, a photo detector has to fulfill various requirements. It must be sensitive in some given spectral region. In some cases, the responsively should be constant or at least well defined within some wavelength range. It can also be important to have zero response in some other wavelength range; an example is solar-blind detectors, being sensitive only to short-wavelength ultraviolet light but not to sun light. The detector must be suitable for some range of optical powers. The maximum detected power can be limited e.g. by damage issues or by a nonlinear response, whereas the minimum power is normally determined by noise. The magnitude of the dynamic range is often most important. The detection bandwidth may begin at 0 Hz or some finite frequency, and ends at some maximum frequency which may be limited by internal processes (e.g. the speed of electric carriers in a semiconductor material) or by the involved electronics.

At present stage of work, the high speed detector (Agilent 81633A). It is an optical power sensor module which can operate in the range from 800 nm to 1700 nm. The InGaAs detector used in the module have power capability of -90dBm to 10dBm.

D. Optical modulator

An optical modulator is a device which can be used for manipulating a property of light beam, e.g. a laser beam. Depending on which property of light is controlled, modulators are called intensity modulators, phase modulators, polarization modulators, spatial light modulators, etc. A wide range of optical modulators are used in very different application areas, such as in optical fiber communications, displays etc.

A pulsed optical source is needed for FLRDS. So a pulse generator of desired frequency is used to modulate the laser. This modulated output is coupled to the loop through a high splitting ratio coupler.

E. Side polished fiber as Evanescent Access Block (EAB)

Side polishing of optical fiber creates a substrate of definable length and depth with parallel surface to guide with virtually zero loss. Fiber side-polishing technology enables access to the evanescent field of the wave propagating in an optical fiber by removing a section of the cladding. Unlike the more common block mounted technology, this approach provides a surface of defined length parallel to the core. The propagation characteristics of the wave can be modified by the structure and material of the replacement cladding. By dynamic modification of structure dimensions, refractive index or absorption, time varying manipulation of the propagation can be achieved in SPF. The evanescent field fibers enable investigation of components and sensing elements.

Chapter 4

4. Theoretical simulations related to FLRDS

4.1. Time domain Analysis

Time domain Analysis is usually based on determining the optical losses within the fibre loop by monitoring the decay lifetime of an optical pulse introduced into the cavity. This decay lifetime is depending on the absorption and scattering losses occurring within the loop and is independent of the intensity fluctuations and detector efficiency. The ringdown time (τ) is related to the round trip time of the loop (t_{rnd}) and transmission per round trip (T) by [51]

$$\tau = \frac{t_{rnd}}{-\ln(T)} \quad (1)$$

The transmission per round trip time (T) is governed by the losses within the fibre loop which includes the losses in the sensor element and the absorption coefficient of fibre (α_{fibre}). Hence much elaborated version of ringdown time is given by [51]

$$\tau = \frac{n L}{c (-\ln(T_{sensor}) + \alpha_{fiber} L)} \quad (2)$$

The transmission T_{sensor} that occurs across the sensor element includes the “undesired” insertion loss and the “desired” loss due to the interaction with the sample [51],

$$-\ln(T_{sensor}) = -\ln(T_{insertion}) + \varepsilon C d \quad (3)$$

where $\ln(T_{insertion})$ is the insertion loss of the sensor element and $\varepsilon C d$ is the Beer-Lambert term which depends on the extinction coefficient (ε), the concentration of the sample (C) and length of the sensing region (d).

There will be single exponential or multi-exponential decay depending on the properties of the system. This multi-exponential decay occurs due to the propagation of light through core, cladding and buffer jacket of the optical fibre. The multi-exponential decay with amplitude a_i and ringdown time τ_i for N decays is given by [51]

$$I(t) = \sum_{i=1}^N a_i \exp\left(-\frac{t}{\tau_i}\right) \quad (4)$$

The amplitude and the ringdown time can be obtained by fitting the loop output to a single or multi-exponential system by using a non-linear least square fitting method.

4.2. Theoretical Simulations related to FLRDS

As per theoretical understanding of FLRDS it is seen that, the decay lifetime depends on the absorption and scattering losses present within the loop. The ringdown time (τ) is related to the round trip time of the loop and transmission per round trip. The simulated plot in Fig. 4.1. shows the ringdown pulse for different loop losses (from 0.05 dB to 0.4 dB). It is observed that, as the loss increases, the ring down time decreases.

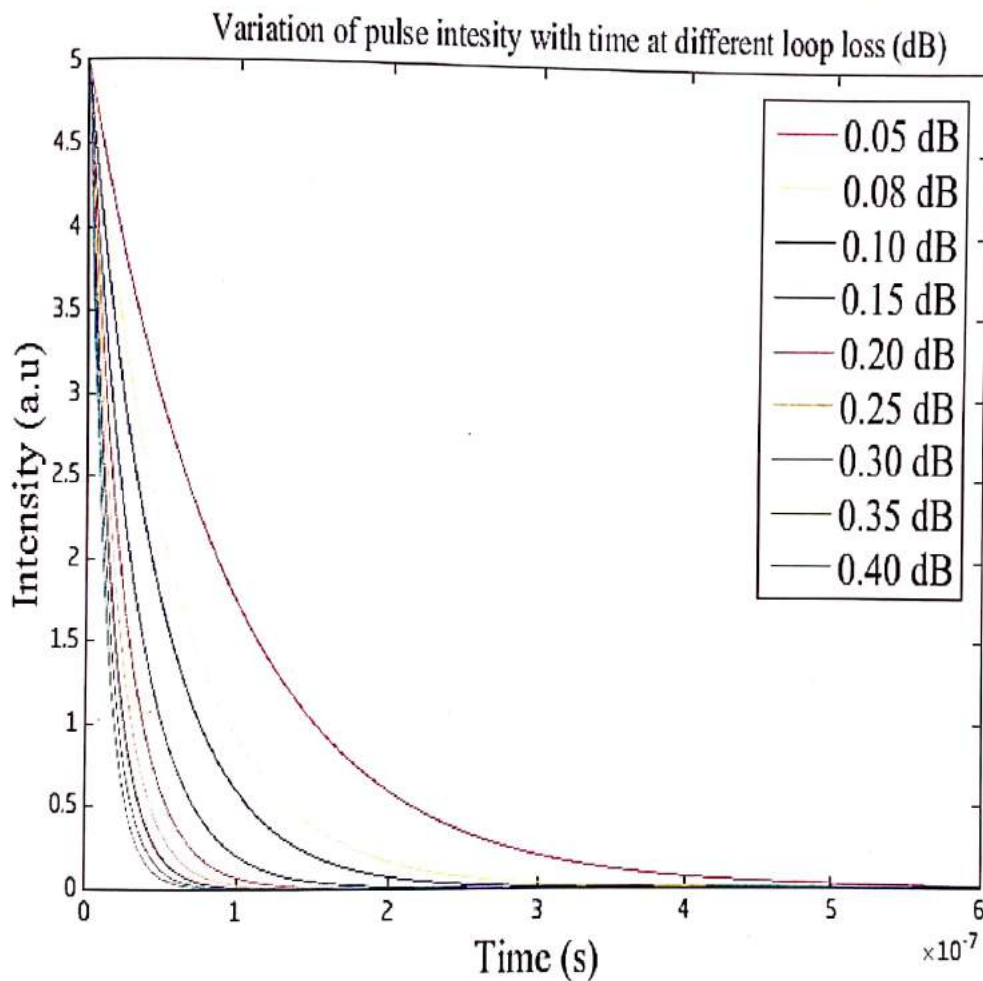


Fig. 4.1. Variation of pulse intensity with time for different loop losses.

The ringdown time corresponding to each loop loss (dB) are both calculated manually and simulated (using MATLAB) for a particular loop length (100m). This is performed from the plot by considering the $1/e^{\text{th}}$ point of the maximum intensity (I_0) of the input pulse. Further this point is extrapolated to the time axis. The calculated and simulated values of RDTs are depicted in a tabular form [Table. 1.].

Table. 1. Simulated values of ring down time corresponding to different loop losses.

Total loss presented in the fiber loop (dB)	The corresponding ring down time (μs)
0.05	9.33
0.08	5.83
0.10	4.67
0.15	3.11
0.20	2.33
0.25	1.87
0.30	1.56
0.35	1.33
0.40	1.17

It can be understood from Table. 1. that the loop loss should be kept as small as possible to get an admissible amount of RDT.

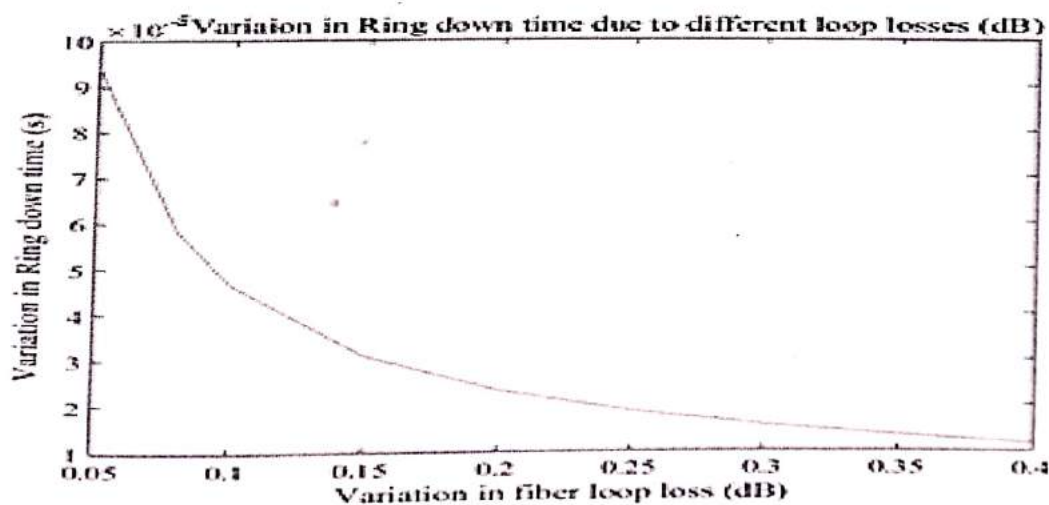


Fig. 4.2. Variation of ringdown time with different loop losses (dB)

The variation of ring down time with various loop losses is presented in the Fig. 4.2 During further designing of any FLRDS set up for practical purpose this plot will help to predict the possible ring down time for particular loop loss within the range 0.05 dB to 0.40 dB.

The number of round trips within the fibre loop is varied for different fibre lengths and the change in intensity is measured. It can be viewed that, as the number of round trip increases the intensity of light decreases exponentially for different fibre loop lengths (for different length of fiber loops 1 m, 3 m and 5 m). The simulated result is illustrated in Fig. 4.3.

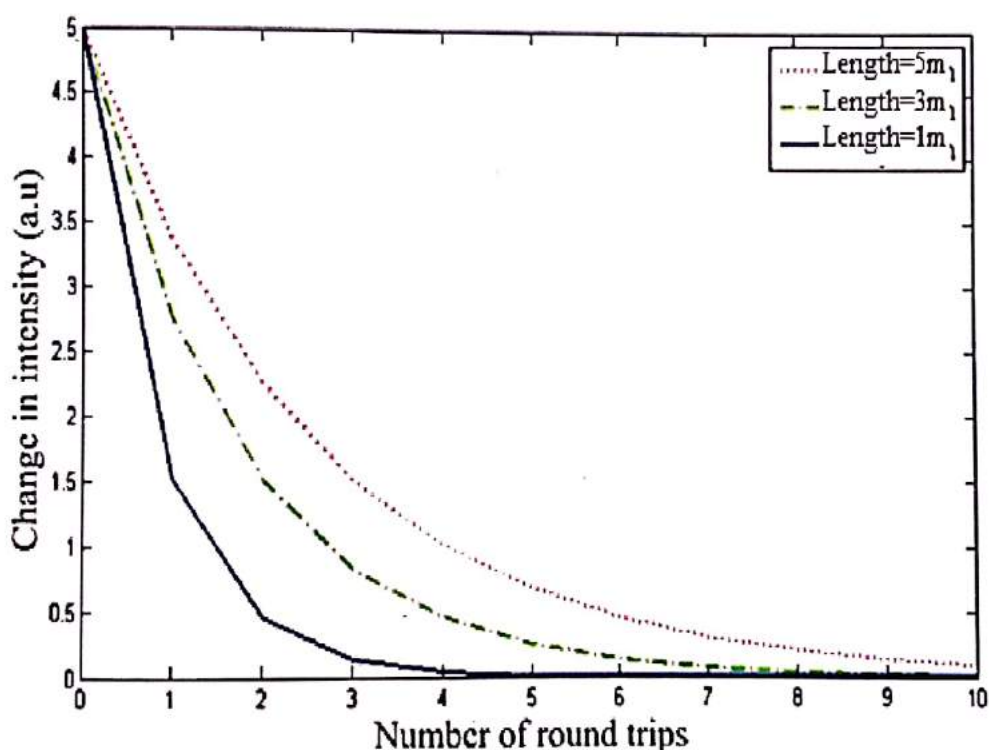


Fig. 4.3. Intensity as a function of number of round trips for different lengths of the loop.

It is perceived that, as the length of the fiber loop increases the intensity of light within the loop decreases, due to various losses occurring in the fiber loop.

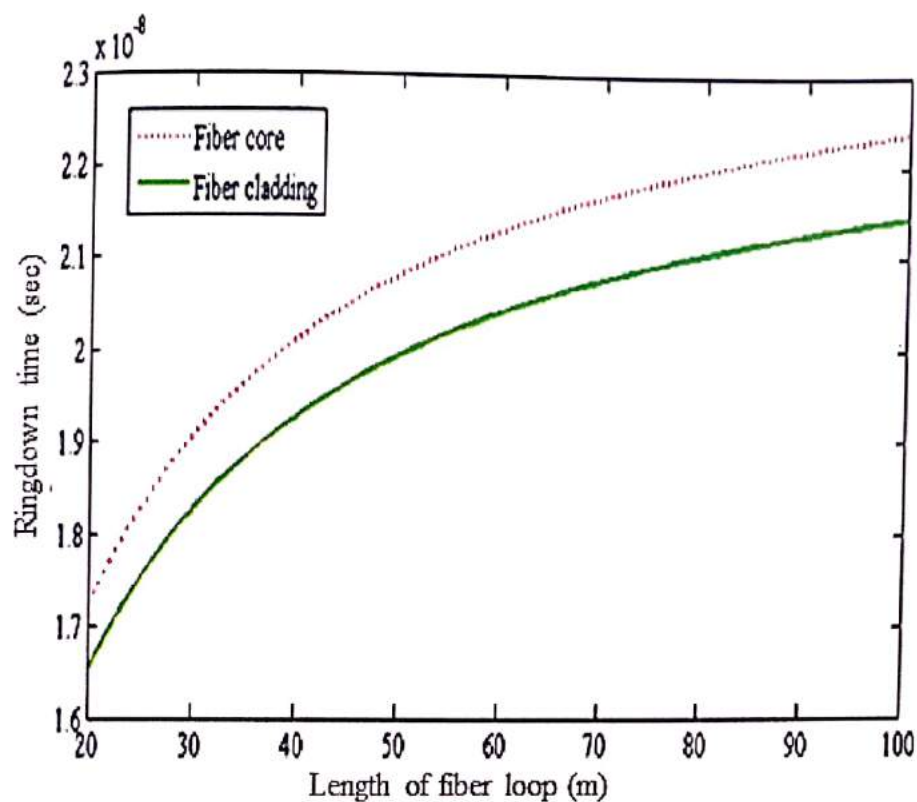


Fig. 4.4. Ringdown time variation indicating the decay rate of core and cladding propagating through the optical fiber.

When a laser pulse is directed into the optical fiber, there will be propagation through the core as well as cladding resulting in a bi-exponential decay. The pulse, that is propagating through the core will be properly guided compared to that of cladding. Hence, the ringdown pulse obtained from the cladding will have more decay rate. The variation of decay rate for core guided and cladding guided pulse is shown in Fig 4.4.

4.3. Effect of Coupler splitting ratio in FLRDS

An FLRDS set up is considered in figure 4, which consists of two couplers, a fiber loop and a sensor head. The couplers used are having splitting ratio of C_1 ($0 < C_1 < 1$) for the first coupler and C_2 ($0 < C_2 < 1$) for the second coupler.

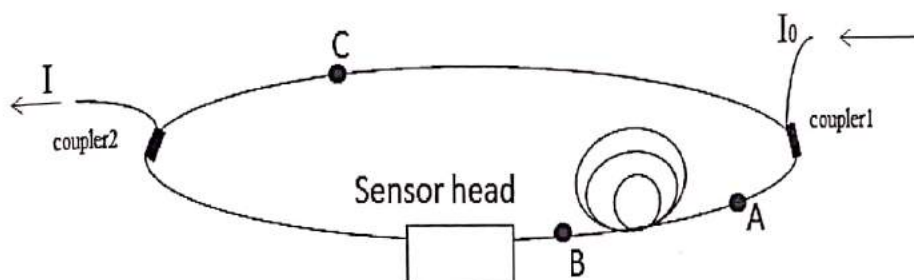


Figure 21. Schematic diagram of FLRDS scheme for analyzing the effect of splitting ratio on the output

The loss incurred in the fiber loop is T_{fiber} and that in the sensor head is T_{sensor} . This T is usually deduced from the attenuation equation which is given by,

$$T = 10 \log \frac{I}{I_0} \quad (5)$$

Where, T represents the total attenuation of the loop, I and I_0 respectively represent the output intensity of laser pulse after propagating through the fiber and initial intensity of the pulse.

So,

$$\frac{I}{I_0} = 10^{\frac{-T}{10}} \quad (8)$$

Then the output intensity is given by equation,

$$I = I_0 10^{\frac{-T}{10}} \quad (9)$$

For the first roundtrip, let I_0 be the intensity of the laser pulse that is provided to the first coupler (C_1), hence the photon intensity at point 'a' is given by,

$$I_a = I_0 (1 - C_1) \quad (10)$$

Then this intensity I_a passes through the fiber loop having a loss of α_1 . So, the photon intensity at point 'b' is represented by,

$$I_b = I_a 10^{\frac{-T_{fiber}}{10}} \quad (11)$$

Similarly it passes through the sensor head having loss T_{sensor} and hence the light intensity at point 'c' is given by,

$$I_c = I_b 10^{\frac{-T_{\text{sensor}}}{10}} \quad (12)$$

Finally the light reaches the second coupler, from where depending on the splitting ratio (C_2) some of the light moves back into the loop and the other to the detector. The light intensity reaching the detector during the first roundtrip I_1 is thus given by,

$$I_1 = I_c (1 - C_2) \quad (13)$$

So, combining all four equations 10, 11, 12, 13,

$$I_1 = I_0 (1 - C_1) (1 - C_2) 10^{\frac{-(T_{\text{fiber}} + T_{\text{sensor}})}{10}} \quad (14)$$

For the second round trip, the light intensity reaching point 'a' is given by,

$$I'_a = I_c C_1 C_2 \quad (15)$$

After considering the same losses at 'b' and 'c' in the optical path, the output light intensity at the detector for the second I_2 is given by,

$$I_2 = I_0 (1 - C_1) (1 - C_2) C_1 C_2 10^{\frac{-2(T_{\text{fiber}} + T_{\text{sensor}})}{10}} \quad (16)$$

Similarly for the third roundtrip, the light intensity I_3 is given by,

$$I_3 = I_0 (1 - C_1) (1 - C_2) (C_1 C_2)^2 10^{\frac{-3(T_{\text{fiber}} + T_{\text{sensor}})}{10}} \quad (17)$$

Finally for n roundtrips the light intensity is given by, [20]

$$I_n = I_0 (1 - C_1) (1 - C_2) (C_1 C_2)^{n-1} 10^{\frac{-n(T_{\text{fiber}} + T_{\text{sensor}})}{10}} \quad (18)$$

Seven round trips of the fiber loop are simulated. The output intensity at the detector for each of the round trip was calculated by taking different splitting ratio, fiber loss ($T_{\text{fiber}} = 0.5 \text{ dB}$) and zero sensor loss ($T_{\text{sensor}} = 0$, i.e. without sensing element) and is tabulated in Table.2.

Table 2. Output intensity of seven roundtrips of the fiber loop without the presence of sensor head in the optical path sensor head

Coupler Ratio	1	2	3	4	5	6	7
C1=99:1 C2=99:1	0.000794 3	0.0006184	0.0004814	0.0003748	0.0002918	0.000227 2	0.0001 769
C1=90:10 C2=90:10	0.0794	0.0511	0.0329	0.0212	0.0136	0.0088	0.0056
C1=98:2 C2=98:2	0.0032	0.0024	0.0018	0.0008463	0.0014	0.0008	0.0006
C1=50:50 C2=50:50	1.9858	0.3943	0.0783	0.0156	0.0031	0.0006	0.0001
C1=90:10 C2=50:50	0.0079	0.0056	0.0040	0.0028	0.0020	0.0014	0.0010
C1=98:2 C2=50:50	0.3972	0.1420	0.0507	0.0181	0.0065	0.0023	0.0008
C1=85:15 C2=85:15	0.0794	0.0156	0.0061	0.0024	0.0009	0.0004	0.0001
C1=80:20 C2=80:20	0.1787	0.0309	0.0120	0.0047	0.0018	0.0007	0.0003
C1=90:10 C2=80:20	0.3177	0.1026	0.0589	0.0338	0.0194	0.0111	0.0064
C1=80:20 C2=75:15	0.0397	0.1615	0.0821	0.0417	0.0212	0.0108	0.0055
C1=75:15 C2=75:15	0.4965	0.2218	0.0991	0.0443	0.0198	0.0088	0.0040

From the tabular column it is observed that, the couplers with splitting ratio 50:50 is having much higher intensity compared to the one with splitting ratios 99:1 and 85:15. After about 3 to 5 rounds, the intensity of 50:50 couplers becomes less, which makes it difficult for detection. Hence it is anticipated that the couplers having splitting ratio 99:1 and 85:15 are providing much satisfactory results compared to others in terms of response. It can be perceived that for about 10 round trips, the intensity from the coupler having splitting ratio 85:15 is higher than the coupler with splitting ratio 99:1. But after that there is an increase in intensity of the output in case of 99:1 coupler, which indicates that it, can allow more number of roundtrips. Until now the optical loop without any sensor head (i.e. $T_{\text{sensor}} = 0$) is considered. But for the selection of a proper coupler the sensor loss which significantly affects the output intensity should also be considered. Next, the fibre loop for different splitting ratios, fibre loss ($T_{\text{fibre}}=1 \text{ dB}$) and sensor loss ($T_{\text{sensor}}=2 \text{ dB}$) is analyzed. About seven round trips were simulated using the MATLAB software and the results are tabulated in Table. 3.

Coupler Ratio	1	2	3	4	5	6	7
C1=0.99,C2=0.99	0.0005012	0.0002462	0.0001209	0.0000594	0.0000292	0.0000143	0.0000070
C1=0.90,C2=0.90	0.0501	0.0203	0.0083	0.0034	0.0014	0.0006	0.0002
C1=0.98,C2=0.98	0.0020	0.0010	0.0005	0.0002	0.0001	0.0001	0.0000
C1=0.50,C2=0.50	1.2350	0.1570	0.0197	0.0025	0.0003	0.0000	0.0000
C1=0.99,C2=0.90	0.0050	0.0022	0.0010	.0004	0.0002	0.0001	0.0000
C1=0.90,C2=0.50	0.2506	0.0565	0.0127	0.0029	0.0006	0.0001	0.0000
C1=0.99,C2=0.50	0.0251	0.0062	0.0015	0.0004	0.0001	0.0000	0.0000
C1=0.98,C2=0.50	0.0501	0.0123	0.0030	0.0007	0.0007	0.0002	0.0000
C1=0.85,C2=0.85	0.1128	0.0408	0.0148	0.0054	0.0019	0.0007	0.0003
C1=0.80,C2=0.80	0.2005	0.0643	0.0206	0.0066	0.0021	0.0007	0.0002
C1=0.75,C2=0.75	0.3132	0.0883	0.0249	0.0070	0.0020	0.0006	0.0002

The tabular column indicates a decrease in number of round trips due to the loss induced by the sensor element. Also the intensity after each round trip obtained at the detector is reduced compared to previous results.

Chapter 5

5. Electrical RC circuit to Model the FLRDS System

Electronic circuit simulation uses mathematical models to replicate the behavior of an actual electronic device or circuit. Simulation software allows for modeling of circuit operation and is an invaluable analysis tool. Due to its highly accurate modeling capability, it is often used by students and researchers for electronics and engineering programs. Electronics simulation software engages the user by integrating them into the learning experience. These kinds of interactive simulation tools actively help to analyze, synthesize, organize and evaluate content and result in improving knowledge.

Simulating a circuit's behavior before actually building it, can greatly improve design efficiency. It actually provides insight into the behavior of electronic circuit designs. In particular, for integrated circuits, the tooling is expensive, breadboards are impractical, and probing the behavior of internal signals is extremely difficult. Therefore, almost all circuit designs relies heavily on simulation. The most well known analog simulator is SPICE (Simulation Program with Integrated Circuit Emphasis). Multisim is one of the few circuit design programs to employ the original Berkeley SPICE based software simulation. Multisim was originally created by a company named Electronics Workbench, which is now a division of National Instruments. Multisim includes microcontroller simulation (formerly known as MultiMCU), as well as integrated import and export features to the Printed Circuit Board (PCB) layout software in the suite, NI Ultiboard. Multisim is widely used in academia and industry for circuit's education, electronic schematic design and SPICE simulation.

In this chapter the optical system of FLRDS has been modeled using Multisim 14.0. This model is found to be very useful as the electronic model of the optical system helped us to design and simulate the circuit. The simulated result is very important for predicting the outcome of the actual experiment. Moreover these simulations will help in designing the practical setup for gas sensing using FLRDS.

Electrical circuits can be used to theoretically simulate the response of optical system to various inputs [5]. In common fiber ring-down spectroscopy, the decay of light is monitored in time. The characteristic ring-down time is dependent on every single decay process, such as transmission at the mirrors, scatter of light at imperfections of the cavity, absorption of the light by the analyte and many more. Each one of these decay processes decreases the light intensity by a certain fraction. If the decay processes work in series, like mirror loss, scatter, and sample absorption, they give rise to a single comprehensive decay process. When there are decay processes that occur simultaneously and independently, such as light decaying in the cladding and in the core of an optical fibre, the overall intensity is given by the sum of all the N -decay process. To model an

exponential optical decay with decay time τ , one can use an RC circuit considering, $\tau = RC$. Consequently, a circuit

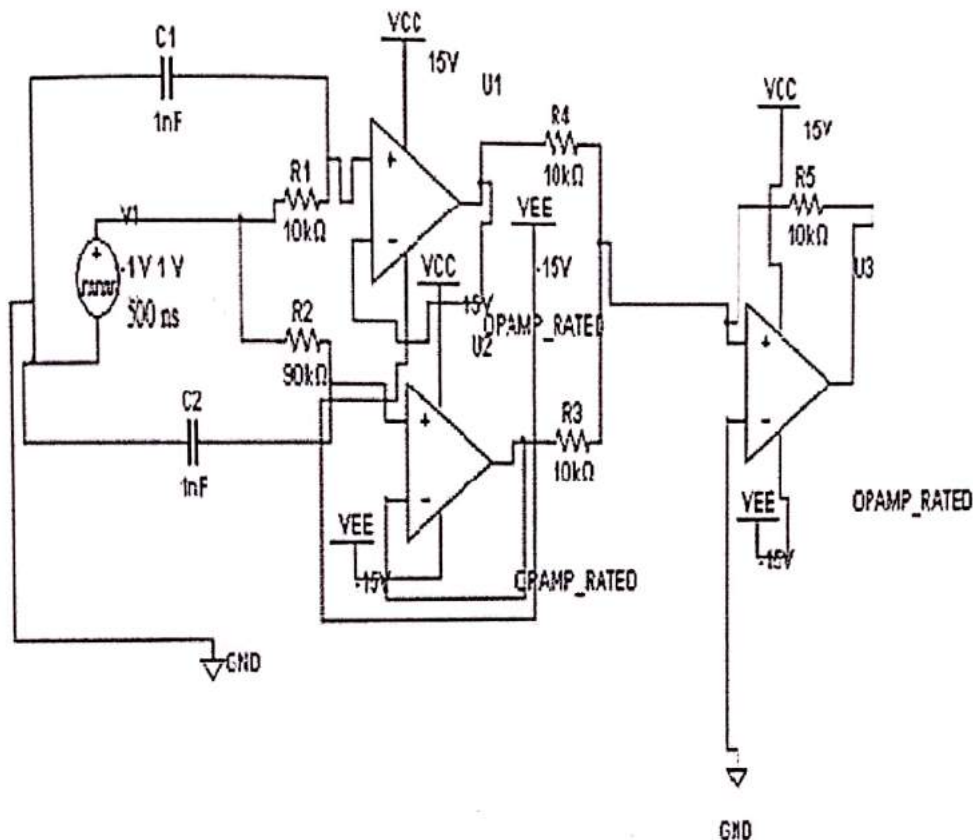


Fig. 5.1. RC circuit diagram of the used bi-exponential circuit with one decay time fixed at 10 μ s (top) and the second one adjusted to 90 μ s (bottom).

containing multiple RC circuits can be summed together, to create a theoretical model for multiple independent optical decay processes, in a fiber ringdown system. R and C values should be chosen to give decay constants that are comparable to typical FLRDS system. Fig. 5.1. shows the circuit diagram for this electrical equivalent to an optical cavity. The circuit is simulated with a squarewave. Here, the operational amplifiers are used as buffer. Buffer generates the output that exactly mirrors the input without introducing any further loss to the entire circuit.

In this case the RDT is approximately as 86 μ s. The theoretically simulated result is depicted in Fig. 8. Since FLRDS is a time domain technique, the simulation of the equivalent electronic circuit is based on transient analysis.

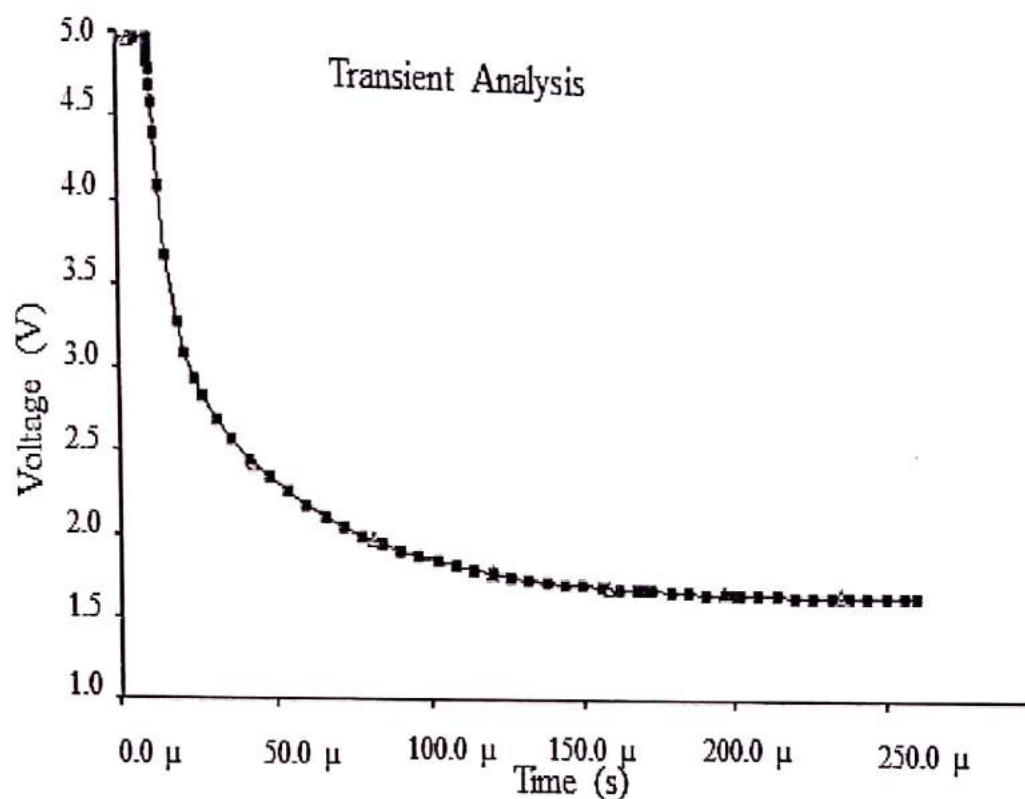


Fig.5.2. Time domain measurement of the input response of the circuit to a square wave simulation.

Chapter 6

6. Proposed setup for Gas sensing using FLRDS

6.1 Introduction

Air pollution is one of the major curses to modern life. It has created global warming and damage to ozone layer which are capable of destroying all our legacies if not prevented as soon as possible. Gas sensors are invented for these purposes. They are able to detect a gas leak and usually have an interface with a control system of the related process to shut it down [1]. They are also capable of detecting combustible and flammable gases. Environmental pollution is basically monitored by reducing the toxic gases (CO_2 , CH_4 , CO, O_3 , NO_x , NH_3 , VOCs, H_2S , HCs, LPG, amines etc) present in the atmosphere mainly due to industrial emissions [1]. For domestic safety purpose detection of poisonous gases from household smoke due to intelligent refrigerator, air conditioning machine or ovens are important. Hence detection of CO_2 , CH_4 , CO etc is essential for household applications of gas sensing. Carbon dioxide is a colourless and odourless gas, whose main source is the motor vehicle and industries. It's the most abundant greenhouse gas in the atmosphere. It traps heat and heavier than air. The main danger with Carbon dioxide is that it can create an Oxygen deficiency and can introduce asphyxiation or suffocation. It enters the body through the lungs from the atmosphere and gets distributed to the blood and causes an acid-base imbalance. Moreover, as CO_2 reduces Oxygen availability, it results rapid breathing, rapid heart rate, clumsiness, convulsions coma and even death. On the other hand it's very important for many agricultural and industrial branches. The possibility of determining the concentration of CO_2 enables one to control various processes and improve safety standards. Agriculture is a field where an appropriate level of CO_2 content in the atmosphere is crucial. In this report a particular form of optical detection technique is described for Carbon dioxide sensing.

6.2 The proposed method and experimental setup for CO₂ sensing using FLRDS

Every gas has a particular absorption wavelength. When energy of that particular wave length is passed through the gas, according to Plank's equation, [equation (1)] some of the molecules gets excited and jumps to the higher energy level.

$$E=h\nu \quad (1)$$

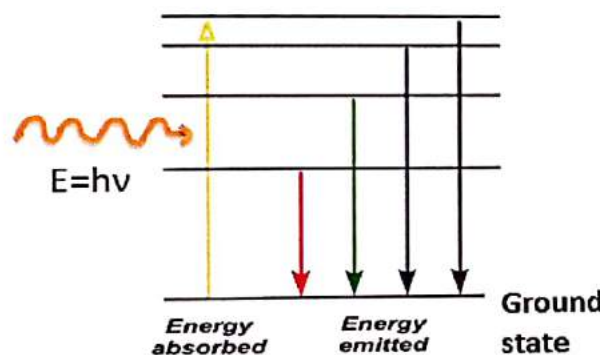


Fig. 6.1. Energy absorption of gas molecules and the corresponding Energy level diagram.

Since the optical absorption is proportional to the gas concentration, it is possible to measure by optical absorption at the specific wavelength. Carbon dioxide shows the highest optical absorption at the mid-infrared (MIR) region [2]. But light sources of MIR cannot be transmitted by optical fibers. The next significant absorption by Carbon dioxide takes place at the wavelength 1572.33 nm. The NIR light can be transmitted by optical fibers (0.2dB/km at 1550nm for single mode fiber). Gas molecules are oscillating around their equilibrium positions. Though the motion of atoms in polyatomic systems due to vibration and rotation appears to be extremely complex, it can be decomposed into elementary movements, the so-called fundamental or normal modes (spinning around an axis, stretching vibration and bending vibration). All normal modes carry a certain, quantized amount of energy. Appropriate energies may induce transitions between ground and excited vibrational states. These transitions carry important information about

the material. Near Infrared Region is the name given to the range in the electromagnetic spectrum between visible light and microwave radiation. Infrared light interacts only with those vibrations whose dipole moment (μ) periodically changes due to the oscillation of the atoms. If the oscillating electromagnetic field of the incident photon couples with the dipole oscillating at the same frequency, it is absorbed. The absorption bands in the NIR spectra correspond to the photon energies used to excite lattice vibrations (phonons).

The optical pulse, which propagates in the ring-down cavity, gets amplified by EDFA in order to compensate the optical losses introduced by the couplers. It also compensates the propagation loss in the single mode fiber (SMF). A band pass filter (BPF) is used to cut the amplified spontaneous emission noise (ASE) usually introduced by EDFA. The FLRD system is already described in the previous section. The proposed setup is to be consisted of a continuous wave (CW) diode laser light source, two fiber couplers, SMF, a photo detector, a mass flow controller (for calibration) and an electronic control. The schematic of the setup is depicted in Fig. 8. [24]. The cross-sections of the cladding and the fiber core of the SMF (SMF-28, Corning, Inc.) are 125 μm and 8.2 μm , respectively. The total optical loss, including absorption loss, fiber connectors' insertion losses and fiber couplers' losses, should be <0.5 dB. The splicing loss is generally estimated by the splicer and depends on each splicing case with a typical value of 0.01–0.03 dB. The port of the second coupler is to be coupled to the InGaAs photo detector (Thorlabs). InGaAs photo detector is to be used because it is sensitive to NIR region. The minimum allowable loop length is determined on the basis of the pulse width to be implemented. Each signal from the CW LASER is applied to a pulse generator to generate a series of square waves. These pulsed series are applied to the diode laser to introduce a pulse into the loop and rapidly drop the laser current to zero.

Therefore, a series of laser pulses are needed to be generated and coupled into the fiber loop, the detector will observe a ringdown signal. For each laser pulse, the detector observes a series of pulsed spikes resulting from each round trip of the laser pulse in the fiber loop. The intensity decay curve will be measured by an oscilloscope which will be interfaced to a computer for further data processing. If an optical pulse width of 500 ns is introduced into the ring down cavity, then the loop length can be considered more than or

equal to 150 m. The proposed measurement technique for the experimental set up is depicted in Fig. 6.2.

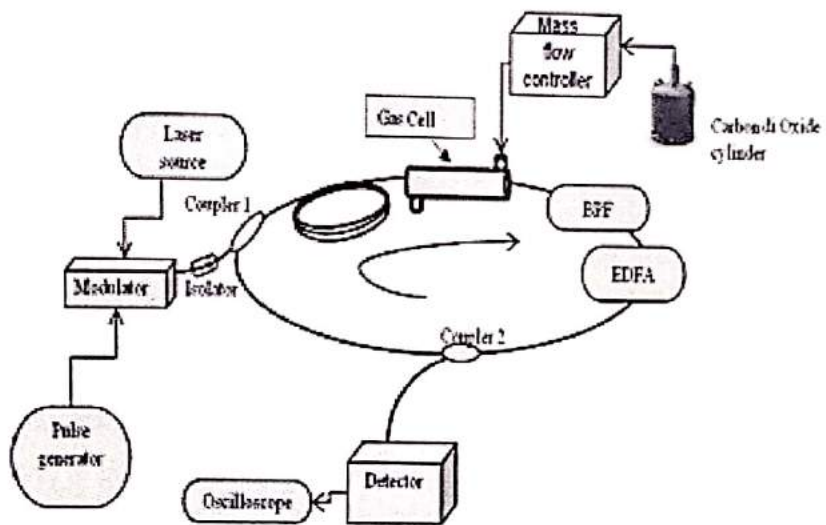


Fig. 6.2. The proposed experimental set up for CO_2 sensing using FLRDS. The sensing mechanism takes place inside the gas cell.

In the experimental set up a mass flow controller (MFC) is introduced for calibration for CO_2 sensing. The gas will pass through the mass flow controller and then get inserted within the sensor head. If the same circuit is implemented and properly executed then it will show reduction of RDT with higher concentration of Carbon-di-Oxide.

Chapter 7

7. Designing and analysis of Transimpedance amplifier for InGaAs Photodetector

7.1. Introduction

Photodiodes (InGaAs Photodiode) convert optical signals into current signal. These signals are usually small in magnitude (nA to μA) in different applications and are commonly amplified by a transimpedance amplifier (TIA) which converts the photocurrent into a proportional output voltage simultaneously amplifying the signal. It is also known as I-to-V converter. An active transimpedance amplifier is based on active elements like BJTs, FETs, and operational amplifier (Op-amp). Transimpedance amplifier using op-amp is the widely used one. Fig. 7.1 shows the active op-amp based transimpedance amplifier circuit with photodiode. In the circuit shown in Fig. 7.1, $+V$ and $-V$ are the supply voltages for the op-amp. and (necessary to maintain stability) are the feedback resistor and feedback capacitor respectively. I_s is the photodiode current. The photodiode is connected between ground and the inverting input of the op-amp. The other input of the op-amp is connected to ground.

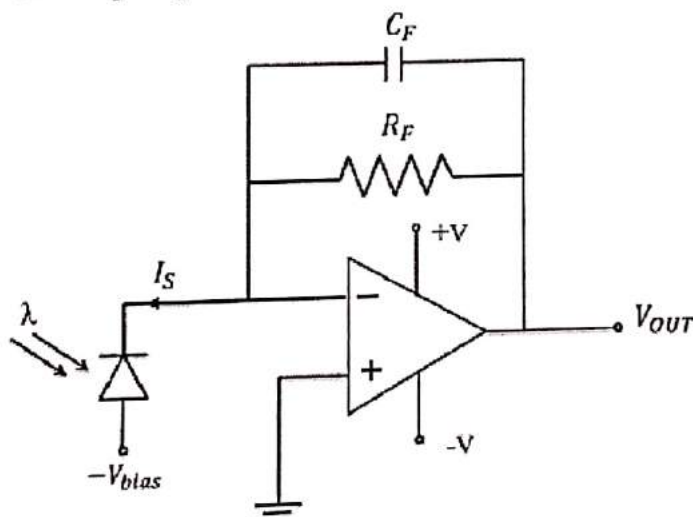


Fig. 7.1 Active op-amp based transimpedance amplifier with photodiode This paper describes the design, implementation and application of TIA for InGaAs photodetector of TPP4NN3 series manufactured by Teradian.

7.2 Design Requirements for the TIA are:

1. Transimpedance gain of at least 10000 V/A
2. -3 dB bandwidth of at least 5 MHz .
3. DC coupling of the photodiode to the TIA.
1. Guaranteed stability with a photodiode capacitance of up to 10 pF .

7.2 DESIGN METHODOLOGY

Methodology adopted here includes selection of various performance parameters for the efficient designing for TIA and selection of suitable op-amp considering the performance parameters.

Gain: The feedback resistor value is used to define the gain of the TIA. For gain to be very high, feedback resistor is made as large as other constraints permit.

Bandwidth: The -3 dB bandwidth of the TIA is inversely proportional to the feedback resistor. Therefore, if the bandwidth is important then, small feedback resistor is used.

Stability: To stabilize the transimpedance amplifier, a large enough capacitor must be placed in parallel with the feedback resistor.

Noise: It is essential to take into account various noise sources (internal and external). Internal noise sources within the op-amp and external noise which the TIA may pick up such as power supply noise.

7.3 SIMULATION

The implementation of TIA coupled with the photodiode characteristics using NI Multisim Software.

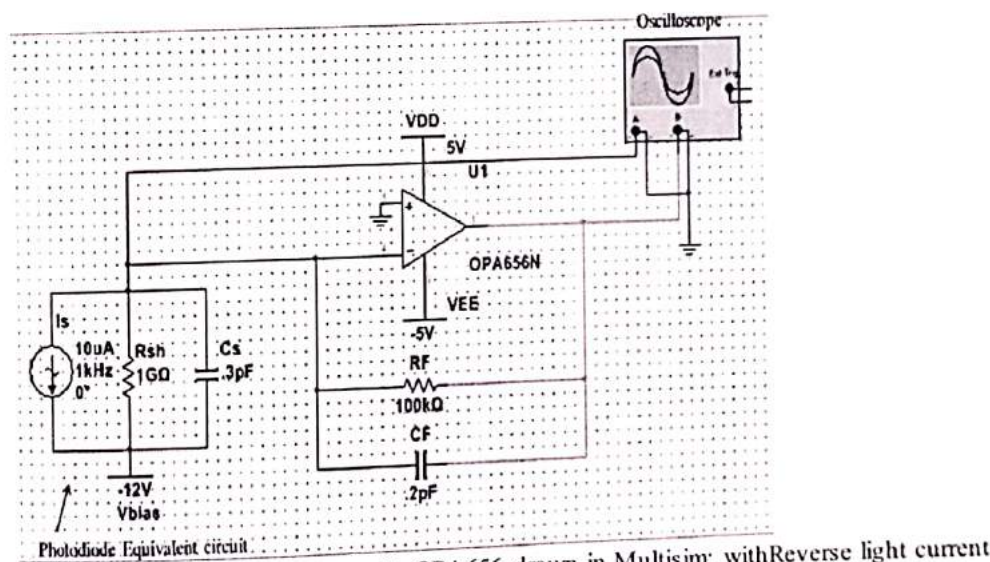


Fig. 7.2. Transimpedance amplifier, with OPA656 drawn in Multisim; with Reverse light current 10 μ A and the feedback resistance 100k Ω

The simulation results are shown in Fig. 7.2. The top graph shows the gain of the TIA in decibels as a function of frequency of the input signal. The -3 dB bandwidth and the gain at -3 dB point are calculated to be 9.61 MHz and 97.02 dB respectively. The bottom graph shows the phase shift as a function of frequency. At -3 dB point, the phase drops to only 117 degrees from 180 degrees and the circuit remains stable.

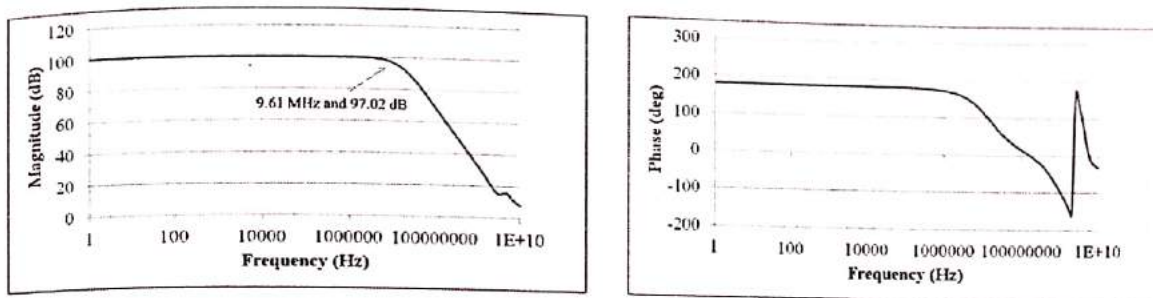


Fig. 7.3. AC analysis (a) gain v/s frequency and (b) phase v/s frequency

Transient Analysis

As we have decided on OPA656 as our preferred op-amp for TIA, we look closely at some of the circuit characteristics. We use the transient analysis to see how the circuit reacts to a specified input signal, and to observe the shape of our output signal. In Figure 4, we can see a typical input response of the transient analysis with OPA656. Our input signal for this analysis is a current signal which has a peak-to-peak value of $20 \mu\text{A}$ with a frequency of 1 kHz

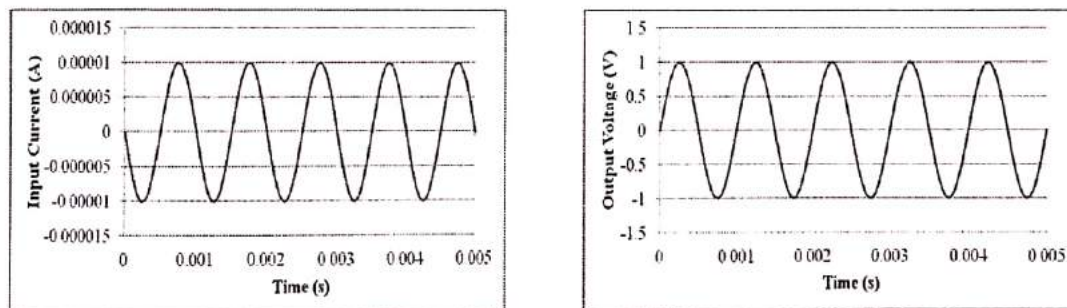


Fig. 7.4 The input and output signal from transient analysis with the selected OPAMP OPA656

So we have designed and simulated a low noise op-amp transimpedance amplifier for InGaAs photodetectors. The presented simulations regarding TIA circuit are performed using NI Multisim 14.0.

Chapter 8

8. CONCLUSION

The training on fibre optics and photonic laboratory is very helpful to acquire the knowledge on preform fabrication, fibre drawing, fibre analysis, Erbium doped fibre amplifiers and other activities of fibre optics sensors.

Initially a literature study and review on different techniques of sensing using FLRDS have been performed. Theoretical studies and analysis have been carried out in detail. MATLAB simulation and Multisim simulation of FLRDS for gas detection is modeled and results are discussed. A detailed study is carried out in various aspects.

In FLRDS, the sensor head is the important part for detecting chemical or gas. The whole optical set present at CGCRI lab is described and studied thoroughly. The required modification to be implemented for gas sensing is also discussed. The optical set up is modeled using electronic circuit simulation software. The model is found to be very useful for prediction of ring down time before starting the experiment. Finally a method as well as a practical set up of Carbon dioxide detection using FLRDS is proposed on the basis of theoretical simulations.

In the last chapter a detailed design and analysis of transimpedance amplifier is presented for extracting the outcome of the optical analysis from the InGaAs photo detector.

Further research

Further I would like to implement the proposed set up and carry on the experiment for detection of Carbon dioxide using nano composite material coated on optical Fiber sensor head.

REFERENCES

- [1] Korotchenkov, G. S. *Handbook of Gas Sensor Materials: Applications Properties, Advantages and Shortcomings for Volume 1: Conventional Approaches*. New York, USA: Springer, 2013.
- [2] Noriyasu, Hiroshi, et al. "Measurement of carbon dioxide concentration by fiber loop ring down spectroscopy for telemetering", Conference on Lasers and Electro-Optics/Pacific Rim Optical Society of America, 2013
- [3] Wang, Chuji, "Fiber loop ringdown sensors and sensing", *Cavity Enhanced Spectroscopy and Sensing*. Springer Berlin Heidelberg, 2014, 411-461.
- [4] Wang, Chuji, "Fiber loop ringdown—a time-domain sensing technique for multi-function fiber optic sensor platforms: current status and design perspectives", *Sensors* 9.10 (2009): 7595-7621.
- [5] Bescherer, K., et al "Measurement of multi-exponential optical decay processes by phase-shift cavity ring-down", *Applied Physics B: Lasers and Optics*, 96.1 (2009): 193-200.
- [6] Waechter, Helen, et al. "Chemical sensing using fiber cavity ring-down spectroscopy", *Sensors* 10.3 (2010): 1716-1742.
- [7] Korotcenkov, Ghenadii. "Handbook of gas sensor materials". Springer New York, 2013.
- [8] Zhao, Yong Lu Bai, Bo Han, and Qi Wang. "Review on Advances of Sensors Based on Fiber Loop RingDown Spectroscopy." *Instrumentation Science & Technology* 41, no. 4 (2013): 349364.
- [9] O'Keefe, Anthony, and David AG Deacon. "Cavity ring- down optical spectrometer for absorption measurements using pulsed laser sources." *Review of Scientific Instruments* 59, no. 12 (1988): 25442551.
- [10] Romanini, Daniele, Irène Ventrillard, Guillaume Méjean, Jérôme Morville, and Erik Kerstel. "Introduction to cavity enhanced absorption spectroscopy." In *Cavity Enhanced Spectroscopy and Sensing*, pp. 160. Springer Berlin Heidelberg, 2014.
- [11] Watson, John. "Fundamentals of photonics: BEA Saleh and MC Teich Wiley Interscience, 1991, pp 966+ xvii ISBN 0471 839 655, £ 56.00." (1992): 177.
- [12] Waechter, Helen, Jessica Litman, Adrienne H. Cheung, Jack A. Barnes, and HansPeter Loock. "Chemical sensing using fiber cavity ringdown spectroscopy." *Sensors* 10, no. 3 (2010): 17161742.
- [13] Gagliardi, Gianluca, and HansPeter Loock, eds. *CavityEnhanced Spectroscopy and Sensing*. London, UK:: Springer, 2014.

- [14] Stewart, George, Kathryn Atherton, Hongbo Yu, and Brian Culshaw. "An investigation of an optical fibre amplifier loop for intracavity and ringdown cavity loss measurements." *Measurement Science and Technology* 12, no. 7 (2001): 843.
- [15] Gupta, Manish, Hong Jiao, and Anthony O'Keefe. "Cavity-enhanced spectroscopy in optical fibers." *Optics letters* 27, no. 21 (2002): 1878-1880.
- [16] Brown, R. Stephen, Igor Kozin, Zhaoguo Tong, Richard D. Oleschuk, and Hans-Peter Loock. "Fiber-loop ring-down spectroscopy." *The Journal of chemical physics* 117, no. 23 (2002): 10444-10447.
- [17] Tong, Zhaoguo, R. Stephen Brown, Hans-Peter Loock, and Richard D. Oleschuk. "Fiber-Loop Ring-Down Spectroscopy for Enhanced Detection of Absorption with Limited Path Length." In *Micro Total Analysis Systems 2002*, pp. 296-298. Springer Netherlands, 2002.
- [18] Vogler, Daniel E., Michel G. Müller, and Markus W. Sigrist. "Fiberoptic cavity sensing of hydrogen diffusion." *Applied optics* 42, no. 27 (2003): 54135417.
- [19] Stewart, George, Kathryn Atherton, and Brian Culshaw. "Cavity enhanced spectroscopy in fiber cavities." *Optics letters* 29, no. 5 (2004): 442444.
- [20] Tarsa, Peter B., Paul Rabinowitz, and Kevin K. Lehmann. "Evanescent field absorption in a passive optical fiber resonator using continuous-wave cavity ring-down spectroscopy." *Chemical Physics Letters* 383, no. 3 (2004): 297-303.
- [21] Tarsa, Peter B., Aislyn D. Wist, Paul Rabinowitz, and Kevin K. Lehmann. "Singlecell detection by cavity ringdown spectroscopy." *Applied Physics Letters* 85, no. 19 (2004): 45234525.
- [22] Wang, Chuji, and Chamini Herath. "High-sensitivity fiber-loop ringdown evanescent-field index sensors using single-mode fiber." *Optics letters* 35, no. 10 (2010): 1629-1631.
- [23] Herath, Chamini, Chuji Wang, Malik Kaya, and David Chevalier. "Fiber loop ringdown DNA and bacteria sensors." *Journal of biomedical optics* 16, no. 5 (2011): 050501050501.
- [24] Noriyasu, Hiroshi, Yuki Fukushima, Takumi Yonekura, and Hiromasa Shimizu. "Measurement of carbon dioxide concentration by fiber loop ring down spectroscopy for telemetering." In *Conference on Lasers and Electro-optics/Pacific Rim*, p. WPF_10. Optical Society of America, 2013.
- [25] Wang, Chuji, and Chamini Herath. "Fabrication and characterization of fiber loop ringdown evanescent field sensors." *Measurement Science and Technology* 21, no. 8 (2010): 085205.
- [26] Zhao, Yong, Lu Bai, and Qi Wang. "Gas concentration sensor based on fiber loop ring-down spectroscopy." *Optics Communications* 309 (2013): 328-332.

Appendix

A. Variation of pulse intensity with time at different loop loss

```
clc;
clear all;
close all;
i0=5;
c=3e0008;
n=1.4;
l=1;
a=0.05;
t=0..000000001:0.0000006;
i=i0*exp((-a*c*t)/((n*l)));
plot(t,i,'r');
hold on;
a=0.08;
i=i0*exp((-a*c*t)/((n*l)));
plot(t,i,'y');
hold on;
a=0.1;
i=i0*exp((-a*c*t)/((n*l)));
plot(t,i,'b');
hold on;
a=0.15;
i=i0*exp((-a*c*t)/((n*l)));
plot(t,i);
hold on;
a=0.2;
i=i0*exp((-a*c*t)/((n*l)));
plot(t,i);
a=0.25;
i=i0*exp((-a*c*t)/((n*l)));
plot(t,i);
hold on;
a=0.3;
i=i0*exp((-a*c*t)/((n*l)));
plot(t,i);
hold on;
a=0.35;
i=i0*exp((-a*c*t)/((n*l)));
plot(t,i);
hold on;
a=0.4;
i=i0*exp((-a*c*t)/((n*l)));
plot(t,i);
hold on;
xlabel('time (s)');
ylabel('intensity');
title('Variation of pulse intensity with time at different loop loss');
```

B. Variation of intensity decay in core and cladding

```
clc;
clear all;
```

```
L=20:100;
c=3e8;
alpha=0.2;
a=alpha.*L;
spliceloss=log(0.2);
n=1.45;
t0=((1.45.*L)./(a-spliceloss)*(1/c));
n1=1.39;
t01=((n1.*L)./(a-spliceloss)*(1/c));
plot(L,t0,'r',L,t01,'g');
```

C. Variation in Ring down time due to different loop losses

```
clc;
clear all;
close all;
i0=5;
c=3e0008;
n=1.4;
l=100;
A=[0.05 0.08 0.10 0.15 0.20 0.25 0.30 0.35 0.40];
rdt=(n*l)./(c.*A);
plot(A,rdt);
hold on;
xlabel('Variation in fiber loop loss (dB)');
ylabel('Variation in Ring down time (s)');
title('Variation in Ring down time due to different loop losses (dB)');
```

D. Ring down time variation with number of round trips

```
clc;
clear all;
close all;
i0=5;
c=3e0008;
n=1.4;
l=0:1:250;
a=0.05;
t=0..0000000001:0.0000006;
t=0.00003;
% i=i0*exp((-a.*c.*t))/((n*l));
i=i0*exp(-(-321.4285714)./l);
plot(l,i,'r');
hold on;
```